Article

Cell Metabolism

Crosstalk between Gut Microbiota and Dietary Lipids Aggravates WAT Inflammation through TLR Signaling

Graphical Abstract

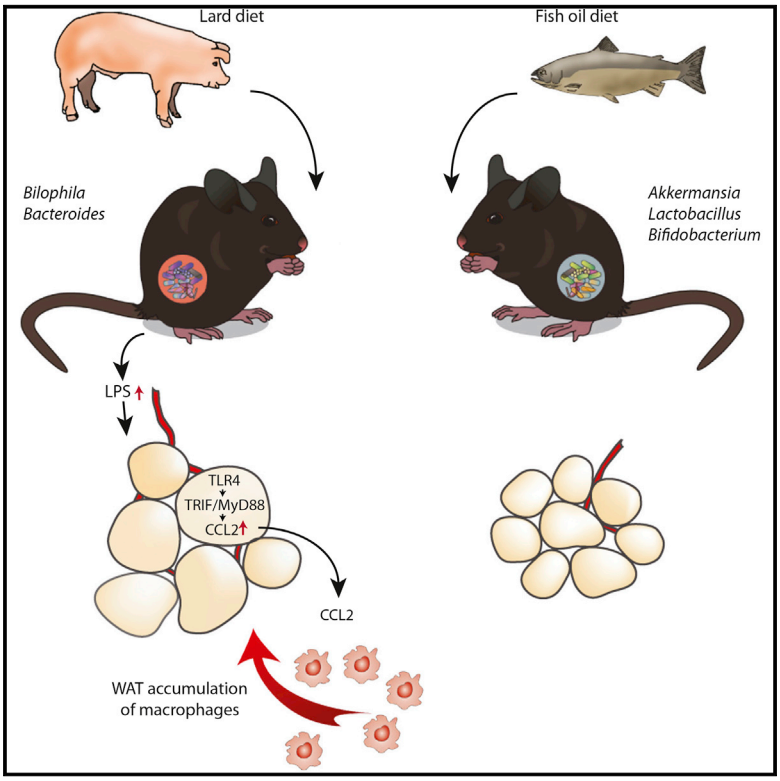

Highlights

- The gut microbiota contributes to phenotypic differences in mice fed lard or fish oil
- Mice lacking MyD88 or TRIF are protected against WAT inflammation
- Microbial-derived factors induce CCL2 in adipocytes through TLR4, MyD88, and TRIF
- Microbial-induced CCL2 enhances macrophage accumulation in WAT

Authors

Robert Caesar, Valentina Tremaroli, Petia Kovatcheva-Datchary, Patrice D. Cani, Fredrik Bäckhed

Correspondence

robert.caesar@wlab.gu.se (R.C.), fredrik.backhed@wlab.gu.se (F.B.)

In Brief

Caesar et al. reveal how saturated lipids in lard affect gut microbial composition to promote obesity and WAT inflammation via TLR signaling and CCL2; in contrast, mice fed a fish-oil diet enriched in polyunsaturated fatty acids are protected. Transfer of microbiota from fish-oil-fed mice dampens lard-induced inflammation.

Accession Numbers

GSE70922

Caesar et al., 2015, Cell Metabolism 22, 658–668
October 6, 2015 ©2015 The Authors
http://dx.doi.org/10.1016/j.cmet.2015.07.026

Crosstalk between Gut Microbiota and Dietary Lipids Aggravates WAT Inflammation through TLR Signaling

Robert Caesar,[1,*] Valentina Tremaroli,[1] Petia Kovatcheva-Datchary,[1] Patrice D. Cani,[2] and Fredrik Bäckhed[1,3,*]
[1]The Wallenberg Laboratory, Department of Molecular and Clinical Medicine, University of Gothenburg, 41345 Gothenburg, Sweden
[2]Université Catholique de Louvain, Louvain Drug Research Institute, Metabolism and Nutrition Research Group, WELBIO (Walloon Excellence in Life Sciences and BIOtechnology), 1200 Brussels, Belgium
[3]Novo Nordisk Foundation Center for Basic Metabolic Research, Section for Metabolic Receptology and Enteroendocrinology, Faculty of Health Sciences, University of Copenhagen, 2200 Copenhagen, Denmark
*Correspondence: robert.caesar@wlab.gu.se (R.C.), fredrik.backhed@wlab.gu.se (F.B.)
http://dx.doi.org/10.1016/j.cmet.2015.07.026

SUMMARY

Dietary lipids may influence the abundance of circulating inflammatory microbial factors. Hence, inflammation in white adipose tissue (WAT) induced by dietary lipids may be partly dependent on their interaction with the gut microbiota. Here, we show that mice fed lard for 11 weeks have increased Toll-like receptor (TLR) activation and WAT inflammation and reduced insulin sensitivity compared with mice fed fish oil and that phenotypic differences between the dietary groups can be partly attributed to differences in microbiota composition. *Trif*$^{-/-}$ and *Myd88*$^{-/-}$ mice are protected against lard-induced WAT inflammation and impaired insulin sensitivity. Experiments in germ-free mice show that an interaction between gut microbiota and saturated lipids promotes WAT inflammation independent of adiposity. Finally, we demonstrate that the chemokine CCL2 contributes to microbiota-induced WAT inflammation in lard-fed mice. These results indicate that gut microbiota exacerbates metabolic inflammation through TLR signaling upon challenge with a diet rich in saturated lipids.

INTRODUCTION

Diets rich in saturated dietary lipids are associated with increased white adipose tissue (WAT) inflammation and metabolic disease (Kennedy et al., 2009), whereas diets rich in polyunsaturated fatty acids have been shown to counteract inflammation and promote a lean and metabolically healthy phenotype (Buckley and Howe, 2009; Calder, 2006; Oh et al., 2010). Host diet also has a major impact on gut microbial composition (Scott et al., 2013), and changes in gut ecology can affect the inflammatory and metabolic properties of the gut microbiota and thereby host physiology (Tremaroli and Bäckhed, 2012). Studies showing that germ-free (GF) mice are protected against diet-induced obesity and exhibit reduced WAT inflammation and insulin resistance (Bäckhed et al., 2007; Caesar et al., 2012; Ding et al., 2010; Rabot et al., 2010) have led to the suggestion that microbial factors may directly contribute to WAT inflammation and adverse metabolic consequences. Circulating microbial factors have, indeed, been identified in healthy humans and mice (Caesar et al., 2010). Furthermore, an increased influx of microbial factors has been linked to inflammation and impaired glucose metabolism through activation of Toll-like receptor (TLR)-dependent signaling (Cani et al., 2007; Henao-Mejia et al., 2012). Several genetic mouse models have shown that deletion of components of the TLR signaling pathway is associated with protection against WAT inflammation and/or rescue of metabolically perturbed phenotypes (Jin and Flavell, 2013). However, although TLR ligands may be of bacterial origin, they may also come from the diet or the host (Yu et al., 2010), and, thus, gnotobiotic models are required to determine how the gut microbiota contributes to WAT inflammation upon diet change.

In the present paper, we aim to determine whether WAT inflammation induced by dietary lipids is mediated through the gut microbiota and to identify molecular mechanisms through which the gut microbiota induces macrophage accumulation in WAT.

RESULTS

Impact of Lard versus Fish-Oil Diet on Gut Microbiota

To assess how the dietary fat sources affects the microbiota, we fed mice isocaloric diets that differed only in fat composition (either lard or fish oil, which are rich in saturated and polyunsaturated lipids, respectively) (Table S1) for 11 weeks. First, we showed that lard-fed mice gained more weight (Figure 1A), consumed more food, and had increased feed efficiency (Figures S1A and S1B) compared with mice fed fish oil. Lard-fed mice had reduced respiratory quotient (RQ) (Figure S1C), indicative of increased fat utilization, both after 2 days and 5 weeks of high-fat diet. The fat source did not change locomotory activity (Figure S1C), but mice fed fish oil utilized more energy for locomotory activity (Figure S1D). As expected, the lard-fed mice had higher fasting insulin and glucose levels, as well as impaired insulin sensitivity, compared to mice fed fish oil (Figures S1E–S1G).

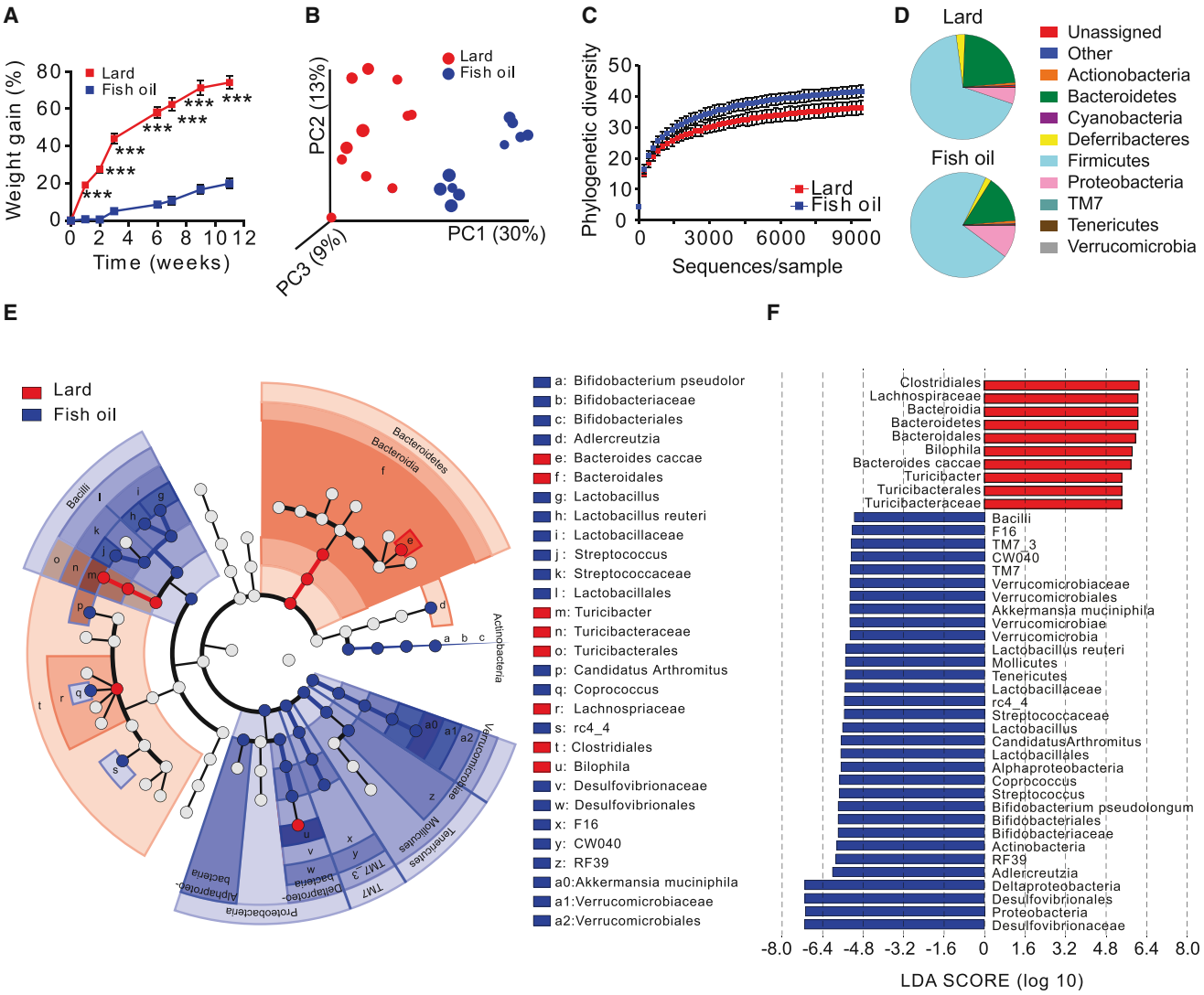

Figure 1. Mice Fed a Lard Diet Have Increased Adiposity and Distinct Gut Microbiota Composition Compared to Mice Fed an Isocaloric Fish-Oil Diet

Mice were fed high-fat diets for 11 weeks.

(A) Body weight gain of mice fed lard or fish oil (n = 15). Data indicate means ± SEM. ***p < 0.001.

(B) Principal coordinate analysis of gut microbiota composition based on unweighted UniFrac in mice fed lard or fish oil (n = 10–11 mice per group).

(C) Rarefaction curves for phylogenetic diversity in microbiota from mice fed lard or fish oil (10–9,410 sequences per sample). Data indicate means ± SD.

(D) Pie charts of gut microbial phyla composition in mice fed lard or fish oil for 11 weeks (n = 9–10 mice per group) (see Table S2 for the list of differentially abundant taxa grouped at the phylum and genus level).

(E) Cladogram generated from LEfSe analysis, showing the most differentially abundant taxa enriched in microbiota from mice fed lard (red) or fish oil (blue).

(F) LDA scores of the differentially abundant taxa shown in (E). Taxa enriched in microbiota from mice fed lard (red) or fish oil (blue) are indicated with a positive or negative LDA score, respectively (taxa with LDA score >2 and significance of $\alpha < 0.05$ determined by Wilcoxon signed-rank test).

See also Table S2.

We analyzed gut microbiota composition by 454 pyrosequencing of the 16S rRNA gene in cecal contents of these mice and observed dramatic changes in the microbial ecology according to the type of dietary fat (Figures 1B–1F; Table S2). Principal coordinate analysis of the unweighted UniFrac showed significant clustering of samples according to diet (Figure 1B), and multivariate non-parametric ANOVA (adonis, 999 permutations) showed that fat source explained about 24% of the variability in microbiota composition ($R^2 = 0.24$, p = 0.001). Diversity within samples was also affected by the type of fat, as shown by a significant decrease in phylogenetic diversity in samples from mice fed lard versus fish oil (Figure 1C; p = 0.001 non-parametric p value calculated using 999 Monte Carlo permutations at the maximum sampled depth). Linear discriminant analysis (LDA) effect size indicated that the genera *Bacteroides*, *Turicibacter*, and *Bilophila* were increased in lard-fed mice, while Actinobacteria (*Bifidobacterium* and *Adlercreutzia*), lactic acid bacteria (*Lactobacillus* and *Streptococcus*), Verrucomicrobia

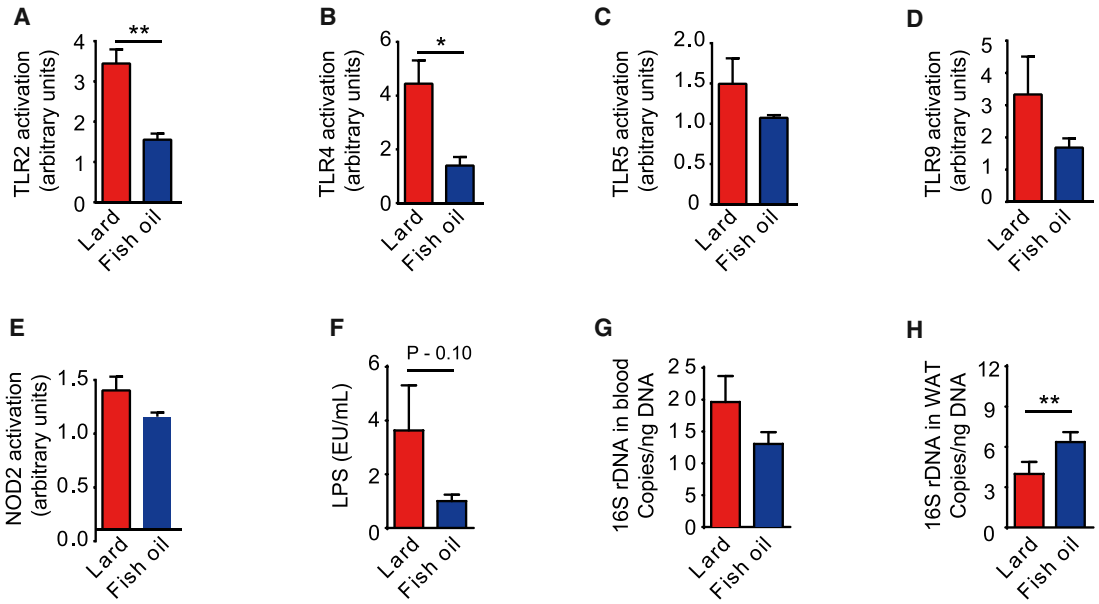

Figure 2. Presence of TLR Ligands, LPS, and Bacterial DNA in Blood and Bacterial DNA in WAT of Mice Fed Lard and Fish Oil

(A–E) Activation of innate immunity receptors induced by stimulation with serum isolated from CONV-R mice fed lard or fish oil for 11 weeks (n = 3).

(F) Concentrations of LPS in serum isolated from CONV-R mice fed lard or fish oil for 11 weeks (n = 11–13 mice per group).

(G) Levels of 16S rDNA in blood from CONV-R mice fed lard or fish oil for 11 weeks (n = 15 mice per group).

(H) Levels of 16S rDNA in WAT from CONV-R mice fed lard or fish oil for 11 weeks (n = 15 mice per group).

Mean values ± SEM are plotted. *$p < 0.05$; **$p < 0.01$.

(*Akkermansia muciniphila*), Alphaproteobacteria, and Deltaproteobacteria were increased in fish-oil-fed mice (Figures 1E and 1F).

Using qPCR, we confirmed the increase in *Akkermansia* and *Lactobacillus* in the cecal contents of mice fed fish oil compared to lard for 11 weeks; we also observed a significant increase in *Lactobacillus*, but not in *Akkermansia*, in fish-oil-fed mice after 3 weeks (Figures S1H and S1I).

Impact of Lard versus Fish-Oil Diet on TLR Activation in Systemic Circulation

Despite the marked differences in the gut microbiota, short-chain fatty acid (SCFA) levels were similar in cecal samples from mice fed lard or fish oil for 11 weeks, with a minor increase only observed for acetate relative to the total SCFAs (C2 C4) in mice fed lard (Figures S2A–S2I). Because it is known that obesity and high-fat diets rich in saturated lipids are associated with increased intestinal absorption of microbial products (Caesar et al., 2010; Cani et al., 2007), we measured the potential of serum from vena cava to activate innate immunity receptors. We found that TLR2 and TLR4—but not TLR5, TLR9, or NOD2—were activated by serum from mice fed lard (Figures 2A–2E), suggesting that a lard diet promotes an increased influx of microbial factors into the systemic circulation. In agreement with these results, we found a trend toward increased levels of the TLR4 ligand LPS (lipopolysaccharide) in mice fed lard for 11 weeks (Figure 2F); however, there was no difference in LPS concentration between mice fed lard and fish oil for 3 weeks (Figure S2J).

Impaired metabolism has been associated with bacterial translocation from the intestine (Amar et al., 2011). Therefore, we determined the levels of bacterial DNA in blood and epididymal WAT using qPCR. We found that the bacterial DNA load was similar in blood samples from mice fed lard or fish oil for 11 weeks (Figure 2G). We observed a small increase in bacterial load in WAT from mice fed fish oil compared to lard, but the levels in both groups were very low (Figure 2H). We profiled the 16S rRNA genes by Illumina sequencing and observed no significant differences in diversity and composition in either blood or WAT between mice fed lard or fish oil for 11 weeks (Figures S3A–S3F). Thus, our data suggest that the gut microbiota impairs glucose metabolism by stimulating inflammation through their pro-inflammatory molecules rather than by translocation from the intestine.

Lard Diet Promotes WAT Inflammation through TLR Signaling

The increased activation of TLR in the systemic circulation of lard-fed mice prompted us to investigate the potential role of TLR signaling in the development of diet-induced WAT inflammation. To test this, we fed lard or fish oil for 11 weeks to mice lacking the TLR adaptor molecules MyD88 or TRIF. As expected, mice fed fish oil gained less body weight and had smaller adipocytes than mice fed lard, regardless of the genotype (Figures 3A–3C). Lard-fed *Myd88*$^{-/-}$ mice were protected against diet-induced obesity and had decreased adipocyte size compared with lard-fed wild-type mice (Figures 3A–3C). By contrast, TRIF deficiency did not affect body weight or adipocyte size upon exposure to lard (Figures 3A–3C).

Fat type had a dramatic effect on WAT inflammation: the number of crown-like structures (CLS; indicative of macrophage abundance in adipose tissue and WAT inflammation) (Cinti et al.,

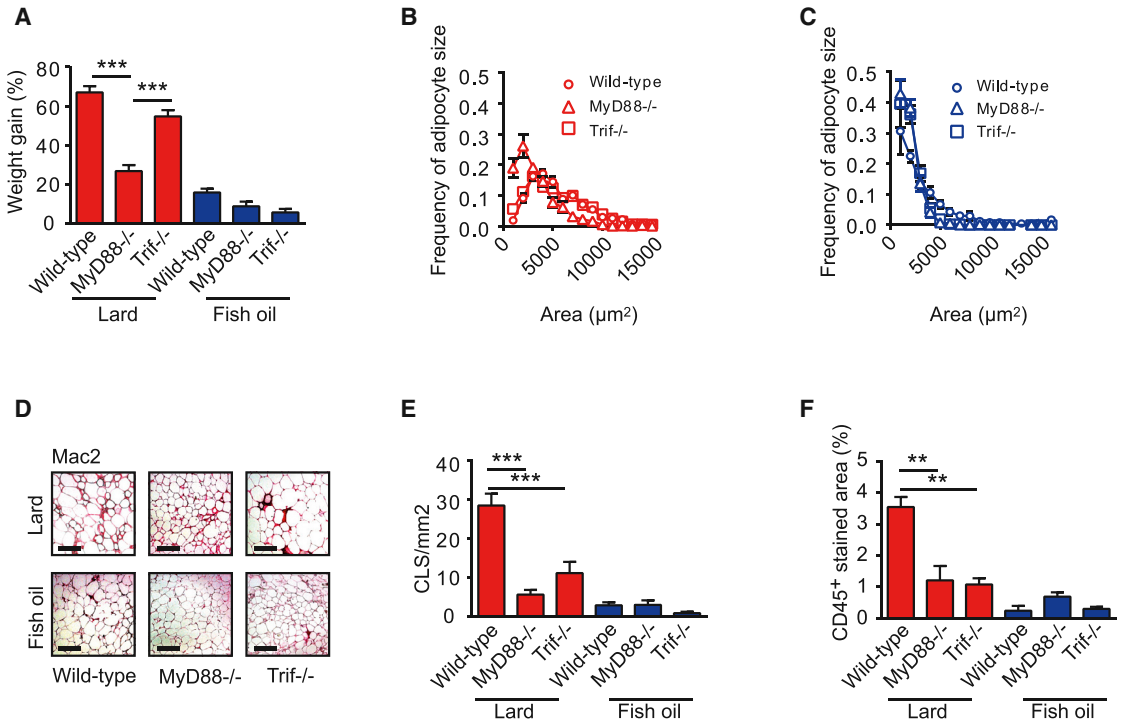

Figure 3. Mice Lacking MyD88 or TRIF Are Protected against Lard-Diet-Induced WAT Inflammation

(A) Body weight gain of wild-type, *Myd88*$^{-/-}$, and *Trif*$^{-/-}$ mice fed lard or fish oil for 11 weeks. ns = 23 (wild-type lard), 7 (*Myd88*$^{-/-}$ lard), 8 (*Trif*$^{-/-}$ lard), 22 (wild-type fish oil), 6 (*Myd88*$^{-/-}$ fish oil), and 9 (*Trif*$^{-/-}$ fish oil).

(B) Distribution of adipocyte sizes in wild-type, *Myd88*$^{-/-}$ and *Trif*$^{-/-}$ mice fed lard (n = 4–6 mice per group).

(C) Distribution of adipocyte sizes in wild-type, *Myd88*$^{-/-}$, and *Trif*$^{-/-}$ mice fed fish oil. n = 8 for wild-type, and n = 4 for *Myd88*$^{-/-}$ and *Trif*$^{-/-}$.

(D) Representative Mac-2 immunostaining of WAT from wild-type, *Myd88*$^{-/-}$, and *Trif*$^{-/-}$ mice fed lard or fish oil. Scale bars, 100 μm.

(E) Quantification of CLS. ns = 7 (wild-type lard), 7 (*Myd88*$^{-/-}$ lard), 5 (*Trif*$^{-/-}$ lard), 7 (wild-type fish oil), 5 (*Myd88*$^{-/-}$ fish oil), and 4 (*Trif*$^{-/-}$ fish oil).

(F) Percentage of area occupied by CD45^{+} cells in WAT of wild-type, *Myd88*$^{-/-}$, and *Trif*$^{-/-}$ mice. ns = 7 (wild-type lard), 7 (*Myd88*$^{-/-}$ lard), 5 (*Trif*$^{-/-}$ lard), 3 (wild-type fish-oil), 4 (*Myd88*$^{-/-}$ fish oil), and 4 (*Trif*$^{-/-}$ fish oil).

Mean values ± SEM are plotted. **p < 0.01; ***p < 0.001.

2005) and accumulation of CD45+ cells (leukocytes) in WAT increased dramatically between 3 and 11 weeks on a lard diet, whereas fish oil did not induce inflammation (Figures S4A and S4B). The numbers of CLS and CD45+ leukocytes were significantly lower in *Myd88*$^{-/-}$ and *Trif*$^{-/-}$ mice than in wild-type mice after 11 weeks on a lard diet (Figures 3D–3F). We also showed that fasting insulin levels were lower and that insulin sensitivity was improved in lard-fed *Myd88*$^{-/-}$ and *Trif*$^{-/-}$ mice compared to lard-fed wild-type mice (Figures S4C–S4F).

These data suggest that dietary saturated fatty acids might mediate WAT inflammation and impaired metabolic phenotypes through TRIF and MyD88 and that the TRIF-mediated effects are independent of the degree of adiposity.

Interaction between Dietary Lipids and the Gut Microbiota Affects WAT Inflammation

Our observation that knockout models for TLR signaling are protected against lard-induced WAT inflammation is consistent with previous reports showing that mice lacking TLR4 have reduced WAT inflammation (Kim and Sears, 2010) and implicates microbial components as mediators of the inflammatory phenotype. To investigate the role of the microbiota in diet-induced WAT inflammation, we fed CONV-R and GF mice lard or fish oil for 11 weeks. Diet had the largest impact on weight gain and lard-fed GF mice gained significantly more weight than fish-oil–fed GF mice (Figure 4A). However, GF mice gained less body weight than their CONV-R counterparts when fed either lard or fish oil (Figure 4A). Increased adiposity, per se, may promote WAT inflammation (Weisberg et al., 2003). Thus, to study the influence of gut microbiota on WAT inflammation independent of differences in adiposity, in subsequent analyses, we used GF and CONV-R mice with matching body weights and equal adipocyte size distribution at the end of the feeding period for each diet (Figures 4B and 4C).

To investigate how dietary lipids and gut microbiota affect WAT inflammation, we performed immunohistochemistry to analyze WAT from CONV-R and GF mice fed a lard or fish-oil diet. As expected, we noted increased numbers of CLS and levels of CD45+ cells in lard-fed versus fish-oil-fed mice, both for CONV-R and GF mice (Figures 4D–4F). Importantly, we also found that the number of CLS was higher in lard-fed CONV-R versus GF mice and a trend (p = 0.08) toward increased levels of CD45+ cells in CONV-R versus GF mice (Figures 4D–4F).

To further investigate how dietary lipids and gut microbiota affect WAT inflammation metabolism, we performed a microarray analysis of WAT from CONV-R and GF mice fed a lard or

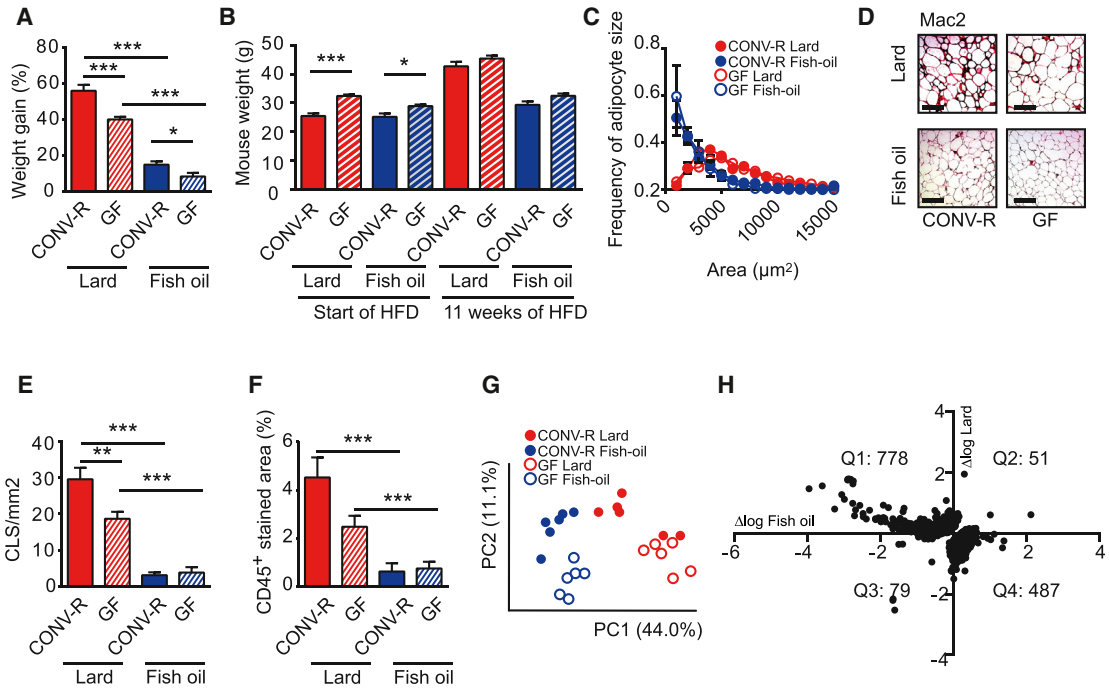

Figure 4. Gut Microbiota and Dietary Lipid Interact to Regulate WAT Inflammation Independent of Body Weight and Adipocyte Size

(A) Body weight gain of CONV-R and GF mice fed lard or fish oil for 11 weeks. ns = 34 (CONV-R lard), 19 (GF lard), 34 (CONV-R fish oil), and 18 (GF fish oil).

(B) Initial and final body weight of mice used for analysis of WAT inflammation (n = 6).

(C) Distribution of adipocyte sizes in mice used for analysis of inflammation and metabolic perturbations. ns = 4 (CONV-R lard), 5 (GF lard), 6 (CONV-R fish oil), and 6 (GF fish oil).

(D) Representative Mac-2 immunostaining of WAT from CONV-R and GF mice fed lard or fish oil. Scale bars, 100 μm.

(E) Quantification of CLS (n = 6 mice per group).

(F) Percentage of area occupied by $CD45^+$ cells in WAT from CONV-R and GF mice fed lard or fish oil (n = 5–6 mice per group).

(G) Principal-component analysis of global gene expression in WAT from CONV-R and GF mice fed lard or fish oil (n = 6 mice per group).

(H) Genes that are regulated by the interaction between diet and gut microbiota. WAT genes induced by the gut microbiota in mice fed lard are plotted on the y axis, and WAT genes induced by the gut microbiota in mice fed fish oil are plotted on the x axis (n = 6 mice per group). Interaction was determined by two-way ANOVA.

Means ± SEM are plotted. *p < 0.05; **p < 0.01; ***p < 0.001.

fish-oil diet. Principal-component analysis of gene expression data revealed that mice separated on diet in the first dimension and on microbial status in the second dimension (Figure 4G). We observed increased expression of genes involved in immune processes and decreased expression of genes involved in energy generation and metabolism in lard-fed versus fish-oil-fed CONV-R mice (Table S3). To compare how the gut microbiota affects WAT gene expression in mice fed lard or fish oil, differences in expression level between CONV-R and GF mice were plotted for significantly regulated genes, with values for mice fed fish oil on the x axis and values for mice fed lard on the y axis (Figure S5). The majority of genes demonstrated a positive linear relationship, indicating that many genes are regulated by the microbiota independently of dietary lipids. Gene ontology analysis showed that the microbiota induced expression of genes involved in, e.g., RNA processing and mitochondrial organization in both dietary groups (Table S4). However, expression of genes involved in immune processes was decreased by the gut microbiota in fish-oil-fed mice and increased by the gut microbiota in lard-fed mice (Table S4). We applied a two-way ANOVA to identify genes with expression levels controlled by the interaction between dietary lipids and gut microbiota (Figure 4H). The subset of these genes located in Q1 (i.e., upregulated by the gut microbiota in lard-fed mice and downregulated in fish-oil-fed mice) was enriched in functional categories associated with immune responses (Table S4). Together, these data suggest that the gut microbiota interacts with dietary lipids to modulate WAT inflammation.

Microbiota from Mice Fed Fish Oil Counteracts Adiposity and Inflammation in Mice Subsequently Fed Lard

To test whether the gut microbiota of mice fed fish oil could attenuate inflammation and protect against diet-induced obesity during lard feeding, we transplanted the cecal microbiota of mice fed fish oil or lard for 11 weeks into recipient mice pretreated with antibiotics and then fed both groups of recipient mice a lard diet for 3 weeks. Strikingly, mice that received fish-oil microbiota gained less weight than mice that received lard microbiota (Figure 5A).

Profiling of the 16S rRNA gene by Illumina sequencing of the cecal contents from the recipient mice demonstrated that the composition of the microbiota differed between mice that received fish-oil or lard microbiota, even though all mice were subsequently fed the same lard diet for 3 weeks. Principal

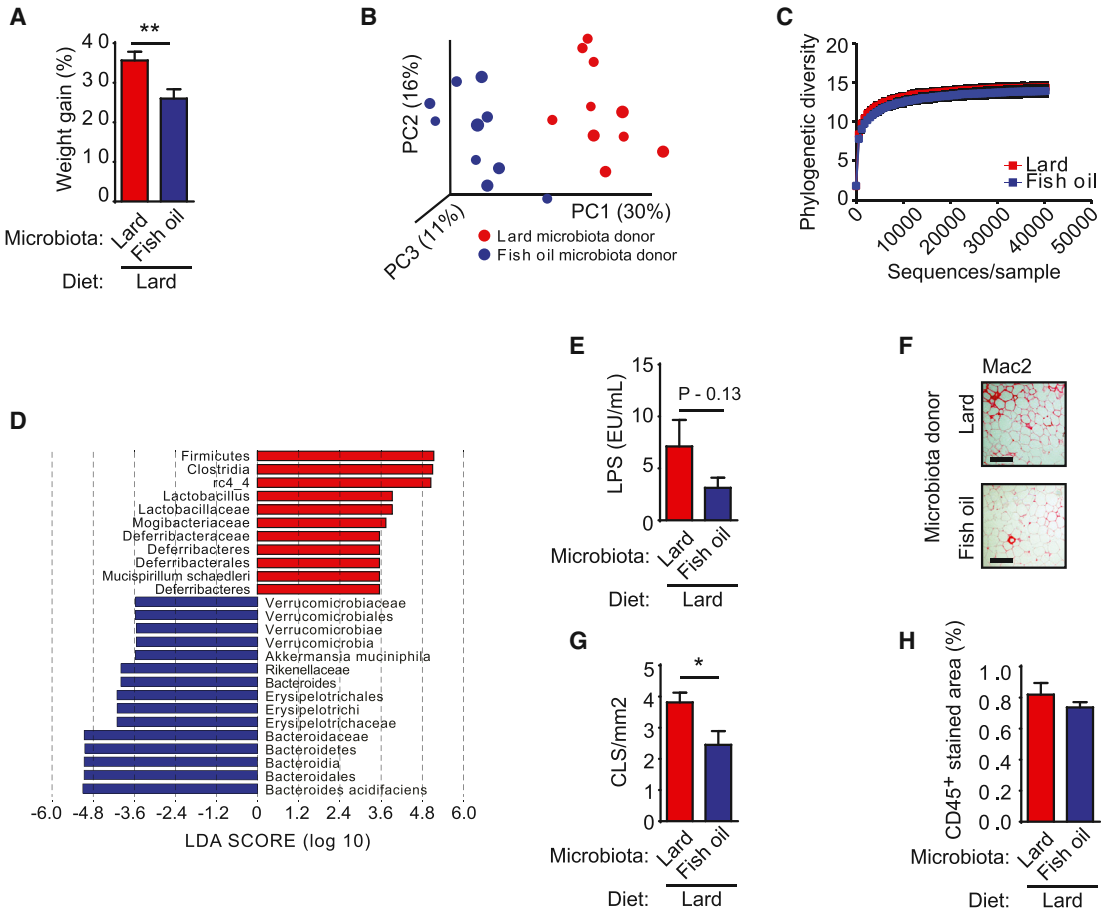

Figure 5. Gut Microbiota Transplanted from Donor Mice Fed a Fish-Oil Diet Counteract Lard-Diet-Induced Adiposity and WAT Inflammation

Mice colonized with gut microbiota from donor mice were fed either a lard or a fish-oil diet for 11 weeks and fed a lard diet for 3 weeks.

(A) Body weight gain (n = 10 mice per group).

(B and C) Indicated here are the (B) principal coordinate analysis of gut microbiota composition based on unweighted UniFrac and (C) rarefaction curves (10–40,610 sequences per sample) for phylogenetic diversity in microbiota (n = 10).

(D) LDA scores of the differentially abundant taxa in blood. Taxa enriched in microbiota from mice fed lard (red) or fish oil (blue) are indicated with a positive or negative LDA score, respectively (taxa with LDA score >2 and a significance of $\alpha < 0.05$ determined by Wilcoxon signed-rank test are shown).

(E) Concentrations of LPS in serum (n = 8–10 mice per group).

(F) Representative Mac-2 immunostaining of WAT. Scale bars, 100 μm.

(G) Quantification of CLS (n = 10 mice per group).

(H) Percentage of area occupied by $CD45^+$ cells (n = 10 mice per group).

Mean values ± SEM are plotted. *p < 0.05; **p < 0.01.

coordinate analysis showed significant clustering of samples according to donor diet (Figure 5B), and multivariate non-parametric ANOVA showed that fat source of the donor explained about 27% of the variability in microbiota composition (R^2 = 0.27, p = 0.001) Within-sample diversity, as measured by phylogenetic diversity, did not differ between the two recipient groups (Figure 5C). Finally, LDA effect size analysis indicated that taxa belonging to *Akkermansia* increased in the cecum of mice that received fish-oil microbiota, while *Lactobacillus* increased in mice that received a lard microbiota (Figure 5D); these results were confirmed by qPCR analysis (Figures S6A and S6B).

We found a trend toward decreased levels of LPS in serum from mice transplanted with microbiota from fish-oil donors (Figure 5E). Analysis of WAT showed that the number of CLS was slightly decreased in mice transplanted with microbiota from fish-oil donors but that the CD45+ cell level was similar in both groups (Figures 5F–5H).

CCL2 in WAT Is Induced by the Gut Microbiota and Mediates WAT Inflammation

To investigate the mechanisms underlying the gut-microbiota-induced WAT inflammation in lard-fed mice, we searched our WAT microarray dataset for differentially regulated genes that are known to be associated with macrophage recruitment. Many previous reports have suggested that the chemokine CCL2 is a mediator of macrophage accumulation in WAT during obesity (Kamei et al., 2006; Kanda et al., 2006; Weisberg et al., 2006). Indeed, we found that *Ccl2* expression in WAT was higher in lard-fed CONV-R mice than in lard-fed GF mice and that both CONV-R and GF mice fed fish oil had low expression of *Ccl2*

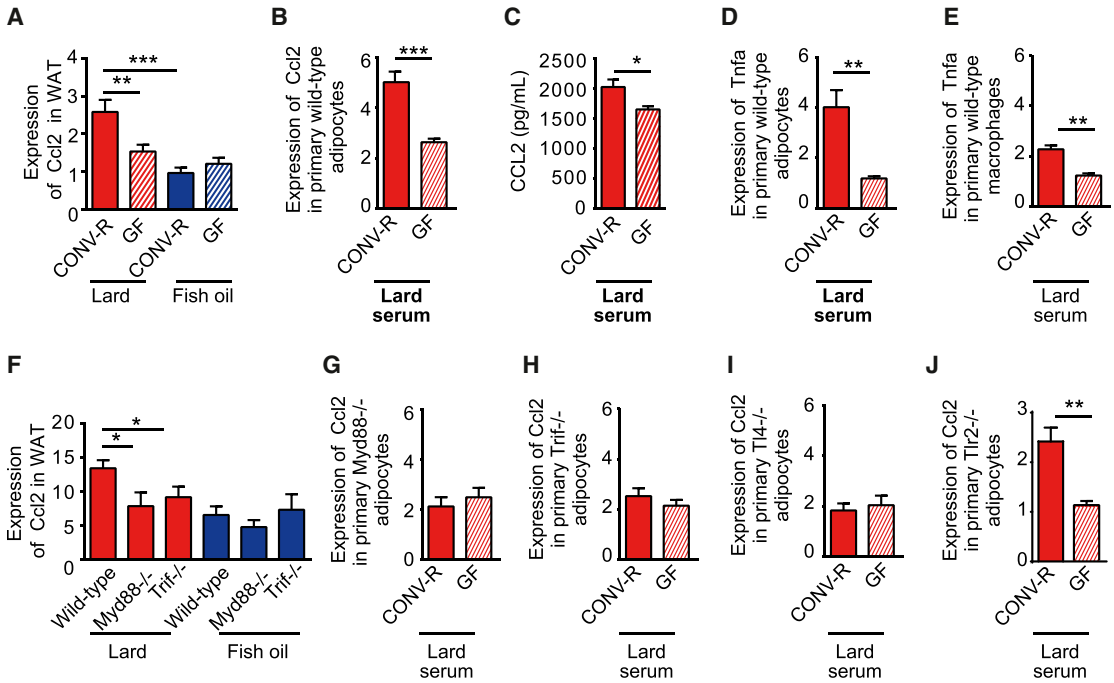

Figure 6. CCL2 Production in WAT Is Induced by the Gut Microbiota through Activation of MyD88, TRIF, and TLR4

(A) Expression of *Ccl2* in WAT from CONV-R and GF mice fed lard or fish oil for 11 weeks (n = 6).

(B) Expression of *Ccl2* in primary adipocytes stimulated for 4 hr with 2% serum from the vena cava of CONV-R or GF mice fed lard (n = 5–6 mice per group).

(C) Secretion of CCL2 from primary wild-type primary adipocytes stimulated for 4 hr with 2% serum isolated from the vena cava of CONV-R and GF mice fed lard (n = 5–6).

(D and E) Expression of Tnfα in primary (D) adipocytes and (E) macrophages stimulated for 4 hr with 2% serum isolated from the vena cava of CONV-R and GF mice fed lard (n = 5–6).

(F) Expression of *Ccl2* in WAT from CONV-R wild-type, *Myd88*$^{-/-}$, and *Trif*$^{-/-}$ mice fed lard or fish oil for 11 weeks. ns = 6 (wild-type lard), 6 (*Myd88*$^{-/-}$ lard), and 4 (*Trif*$^{-/-}$ lard).

(G–J) Expression of *Ccl2* in (G) *Myd88*$^{-/-}$, (H) *Trif*$^{-/-}$, (I) *Tlr4*$^{-/-}$, and (J) *Tlr2*$^{-/-}$ primary adipocytes stimulated for 4 hr with 2% serum isolated from the vena cava of CONV-R or GF mice fed lard (n = 5–6).

Mean values ± SEM are plotted. *p < 0.05; **p < 0.01; ***p < 0.001.

(Figure 6A). Because the WAT microarray dataset is from GF and CONV-R mice with matching body weights (as shown in Figures 4B and 4C), the difference in *Ccl2* expression between lard-fed CONV-R and GF mice was independent of body weight and adipocyte size.

To test the hypothesis that factors in the serum of lard-fed CONV-R mice promote inflammation in WAT, primary adipocytes and macrophages were exposed to serum from CONV-R or GF mice fed lard. Gene expression and secretion of CCL2 were increased in adipocytes, but not macrophages, treated with serum from lard-fed CONV-R mice compared to cells treated with serum from lard-fed GF mice (Figures 6B and 6C; Figures S7A and S7B). We showed that treatment with serum from lard-fed CONV-R mice increased expression of *Tnfα* in both adipocytes and macrophages (Figures 6D and 6E), indicating that circulating microbial factors may trigger a general inflammatory response in both these cell types.

To study the role of innate immunity signaling in the regulation of *Ccl2*, we analyzed *Ccl2* expression in WAT from *Myd88*$^{-/-}$ and *Trif*$^{-/-}$ mice fed lard or fish oil. *Ccl2* expression was lower in WAT from lard-fed *Myd88*$^{-/-}$ and *Trif*$^{-/-}$ mice than that from lard-fed wild-type mice, while *Ccl2* expression in mice fed fish oil was low regardless of genotype (Figure 6F). We also showed that *Ccl2* expression was not increased when primary *Myd88*$^{-/-}$, *Trif*$^{-/-}$, or *Tlr4*$^{-/-}$ adipocytes were exposed to serum from lard-fed CONV-R mice compared to adipocytes treated with serum from GF mice (compare Figures 6G–6I with 6B). In contrast, *Ccl2* expression in primary *Tlr2*$^{-/-}$ adipocytes was increased by exposure to serum from lard-fed CONV-R mice compared to exposure to serum from GF mice (Figure 6J). These data indicate that there are factors present in the blood of CONV-R mice that induce *Ccl2* expression through pathways involving TLR4, MyD88, and TRIF but not TLR2.

To investigate whether CCL2 is involved in the development of WAT inflammation induced by the gut microbiota and lard diet, GF mice were conventionalized and fed a lard diet for 4 weeks in the presence of either the CCL2 inhibitor mNOX-E36 or the nonfunctional control substance revmNOX-E36. Mice treated with mNOX-E36 and revmNOX-E36 did not differ in body weight or adipocyte size (Figures 7A and 7B). Strikingly, however, conventionalized mice treated with mNOX-E36 had decreased abundance of CLS and CD45+ cells in WAT compared to mice treated with revmNOX-E36 (Figures 7C–7E), indicating a role of CCL2 in macrophage recruitment to WAT.

Taken together, these data suggest that CCL2 is induced by factors in the blood of CONV-R mice fed a lard diet through

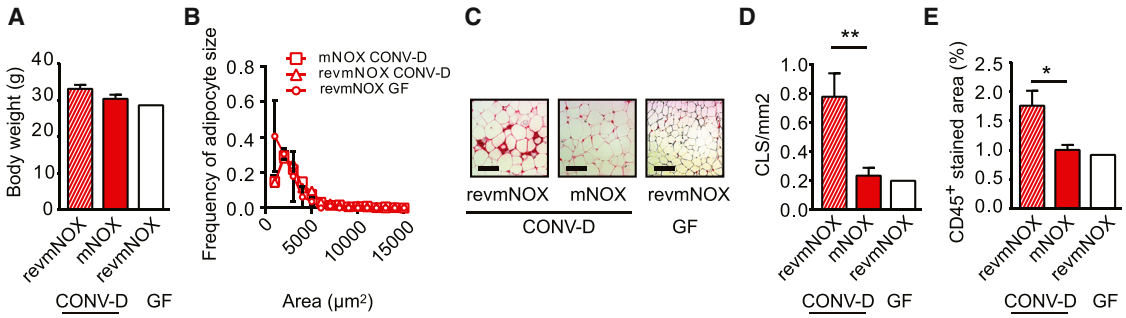

Figure 7. CCL2 Mediates WAT Inflammation

(A and B) Indicated here are the (A) body weight and (B) distribution of adipocyte size in WAT from CONV-D mice fed lard for 28 days and treated with either revmNOX or mNOX and from GF mice fed lard for 28 days and treated with revmNOX. n = 8 (CONV-D revmNOX and CONV-D mNOX), and n = 2 (GF revmNOX).

(C) Representative Mac-2 immunostaining of WAT from CONV-D mice fed lard and treated with either revmNOX or mNOX and from GF mice fed lard and treated with revmNOX. Scale bars, 100 μm.

(D and E) Indicated here are the (D) quantification of CLS and (E) percentage of area occupied by $CD45^+$ cells in WAT from CONV-D mice fed lard and treated with either revmNOX or mNOX and from GF mice fed lard and treated with revmNOX. n = 8 (CONV-D revmNOX and CONV-D mNOX), and n = 2 (GF revmNOX). Mean values ± SEM are plotted; *$p < 0.05$; **$p < 0.01$.

mechanisms involving MyD88, TRIF, and TLR4 and that CCL2 facilitates accumulation of macrophages in WAT.

DISCUSSION

In the present study, we demonstrate that the type of dietary lipids affects the gut microbiota and that the gut microbiota contributes to the phenotypic differences between mice fed lard and mice fed fish oil. Mice fed a lard diet have increased TLR activation in the systemic circulation, increased WAT inflammation, and impaired insulin sensitivity compared to mice fed fish oil. We found that mice lacking MyD88 or TRIF are protected against lard-induced WAT inflammation and metabolic perturbations and that saturated dietary lipids and the gut microbiota interact to induce WAT inflammation. In addition, we show that CCL2 is required for microbiota-induced macrophage recruitment to WAT in mice on a lard diet and that expression of CCL2 in adipocytes is induced by factors in the blood of lard-fed CONV-R mice through a mechanism involving MyD88, TRIF, and TLR4.

We showed that the type of dietary fat is a major driver of community structure, affecting both the composition and diversity of the gut microbiota. Results from 454 pyrosequencing and qPCR showed that mice fed fish oil had increased levels of taxa from the genera *Lactobacillus*, a known probiotic that has been linked to reduced inflammation and mucosal lesion scores in several models of inflammatory bowel diseases (Guarner et al., 2005), and *Akkermansia muciniphila*, which has been shown to reduce fat mass gain and WAT macrophage infiltration and improve gut barrier function and glucose metabolism when administered to mice with diet-induced obesity (Everard et al., 2013). By contrast, mice fed lard had increased levels of taxa related to *Bilophila*. Previous studies have shown that *Bilophila* increases in mice and humans after consumption of diets rich in saturated fats of animal origin (David et al., 2014; Devkota et al., 2012), and *Bilophila wadsworthia* has been shown to exacerbate colitis in genetically susceptible models (Devkota et al., 2012).

To determine whether the microbiota of fish-oil-fed mice could confer protection against lard-diet-induced adiposity and inflammation, we transplanted microbiota from lard- or fish-oil-fed mice into antibiotic-treated mice that were then fed a lard diet for 3 weeks. Here, we used antibiotic-treated mice rather than GF mice because it is known that GF mice have an underdeveloped immune system (Hooper et al., 2012), which could potentially confound this analysis. Mice that received microbiota from a lard-fed donor showed increased adiposity and inflammation, together with a significant increase in *Lactobacillus*, compared to mice that received microbiota from a fish-oil-fed donor. Therefore, these data do not provide evidence for a role of *Lactobacillus* in reducing inflammation. However, we found that the enrichment of *Akkermansia* co-occurred with partial protection against adiposity and inflammation in mice transplanted with fish-oil microbiota and fed a lard diet, highlighting *Akkermansia* as a potential mediator of the improved inflammatory and metabolic phenotype of mice fed fish oil. This finding is in agreement with previous findings linking *Akkermansia muciniphilia* with protection to diet-induced obesity (Everard et al., 2013; Shin et al., 2014).

Serum from mice fed lard had increased capacity to activate TLR4, which has been linked to WAT inflammation and metabolic perturbations (Caesar et al., 2012; Cani et al., 2007; Creely et al., 2007). Furthermore, we found that mice deficient in either of the two TLR adaptor molecules MyD88 and TRIF were protected from lard-induced WAT inflammation and insulin sensitivity. These findings are consistent with earlier studies showing reduced inflammation in mouse models lacking functional MyD88 (Björkbacka et al., 2004; Everard et al., 2014; Michelsen et al., 2004) or TRIF (Richards et al., 2013). One report has shown that MyD88 protects against glucose homeostasis perturbations and liver disease during a high-fat diet (Hosoi et al., 2010). Inconsistencies in reports on the role of MyD88 may be due to environmental factors at different animal facilities. For example, the presence of segmented filamentous bacteria, which are enriched in *Myd88*$^{-/-}$ mice (Larsson et al., 2012) and have a major impact on host immunity (Ivanov et al., 2009), differs between animal facilities (Kriegel et al., 2011). Importantly, the TRIF-deficient mice in our study had the same

body weight and adipocyte size as the wild-type mice, showing that protection against WAT inflammation was not dependent on reduced adiposity.

TLR signaling can be activated by both microbial and endogenous ligands, and some investigators have suggested that saturated fatty acids promote inflammation and insulin resistance in obesity through TLR4 (Shi et al., 2006). The gut microbiota modulates host lipid metabolism (Velagapudi et al., 2010); therefore, protection against WAT inflammation in *Myd88*$^{-/-}$ and *Trif*$^{-/-}$ mice fed lard might be due to decreased TLR signaling induced by ligands originating from the host or from the diet. Here, we showed that serum levels of LPS were higher in mice fed lard compared to mice fed fish oil, indicating that microbial factors are present in the periphery that may directly affect WAT inflammation. However, we cannot exclude the possibility that other factors, such as saturated lipids, also directly contribute to the inflammatory response by activating TLR signaling (Huang et al., 2012). Furthermore, to determine the specific impact of the gut microbiota on lard-induced WAT inflammation, we compared the effects of lard and fish oil in CONV-R versus GF mice. As expected, GF mice were partly protected against lard-induced WAT inflammation, although the protection against obesity in GF mice was less than that observed in previous studies (Bäckhed et al., 2007; Caesar et al., 2012; Ding et al., 2010; Rabot et al., 2010). This is likely due to the reduced sucrose levels in the high-fat diets used in the present study. Sucrose levels have previously been shown to have a major impact on microbiota-induced obesity (Fleissner et al., 2010). We used this fact to our benefit, as we could use weight-matched mice to try and untangle whether the microbiota modulated WAT inflammation by weight-dependent or -independent mechanisms. Importantly, we observed an adiposity-independent link between the gut microbiota and WAT inflammation, which may implicate microbially derived products as mediators of inflammation through TLRs. However, we also showed that GF mice fed lard had increased WAT inflammation compared to GF mice fed fish oil, indicating that microbiota-independent mechanisms also contribute to accumulation of immune cells in WAT.

Previous studies have demonstrated that gut-microbiota-derived factors can induce inflammation and *Tnfα* expression in WAT (Caesar et al., 2012; Cani et al., 2007), and we showed that serum from lard-fed CONV-R mice compared to GF mice had an increased capacity to induce expression of *Tnfα* in both adipocytes and macrophages. CCL2 is the only chemokine that has been shown to mediate inflammation in a WAT-specific knockout model (Lee and Lee, 2014), and TLR ligands have been shown to induce secretion of CCL2 from 3T3-L1 adipocytes (Kopp et al., 2009). Here, we found that *Ccl2* expression in primary adipocytes and WAT was induced by microbial factors in serum and required the presence of MyD88, TRIF, and TLR4. Overexpression of *Ccl2* in adipocytes has been shown to result in WAT inflammation and insulin resistance without obesity (Kamei et al., 2006; Kanda et al., 2006), and mice deficient in CCL2, or its receptor chemokine (C-C motif) receptor 2 (CCR2), have reduced WAT inflammation and insulin resistance during a high-fat diet (Kanda et al., 2006; Weisberg et al., 2006). A recent study also reported that CCL2 promotes local proliferation of macrophages in WAT (Amano et al., 2014). By using the specific pharmacological CCL2 inhibitor mNOX-E36 (Kulkarni et al., 2007, 2009; Wlotzka et al., 2002), we demonstrated that CCL2 is essential for WAT macrophage accumulation in our model and, therefore, constitutes a putative mediator of gut-microbiota-induced WAT inflammation. In addition, we found that GF mice fed lard or fish oil had similar expression levels of *Ccl2* in WAT, suggesting that microbiota-independent WAT inflammation is not mediated through CCL2.

Taken together, our data show that interaction between the gut microbiota and dietary lipids induces WAT inflammation. We also identify putative mechanisms, including the role of cell signaling components and regulation of chemokine expression. The study establishes the gut microbiota as an independent factor aggravating inflammation during diet-induced obesity and, therefore, a suitable target for therapies against associated metabolic perturbations.

EXPERIMENTAL PROCEDURES

Wild-type C57Bl/6, *Myd88*$^{-/-}$, and *Trif*$^{-/-}$, *Tlr4*$^{-/-}$, and *Tlr2*$^{-/-}$ mice were maintained under standard specific-pathogen-free (SPF) or GF conditions as described previously (Caesar et al., 2012). All mice were males and 11–14 weeks of age at the start of the experiments. Mice were weight matched at the start of the experiments, except when the aim was to compare weight-matched mice at the end of the experiment as indicated in the text. Mice were fed irradiated isocaloric diets (45% kcal fat) of identical composition except for the source of fat, which was either menhaden fish oil (Research Diets, D05122102) or lard (Research Diets, D10011202) (Table S1), for 11 weeks unless otherwise indicated. The mice were fasted for 4 hr before they were killed. Blood samples and epididymal WAT samples were harvested at the end of the experiment. Weekly food consumption was measured cage-wise.

To study the role of CCL2 in WAT inflammation during conventionalization, three groups of GF mice were injected subcutaneously with 20 mg/kg of the CCL2 inhibitor mNOX-E36 (Baeck et al., 2012) or the nonfunctional control substance revmNOX-E36 (both NOXXON Pharma) three times per week for 30 days. From day 3, the mice were fed a lard diet, and two groups of mice (one group receiving mNOX-E36 and the other receiving revmNOX-E36) were transferred to a conventional environment and gavaged with cecal content (isolated from a SPF 12-week-old male C57Bl/6 mouse) suspended in 200 μl PBS. The third group of mice (receiving revmNOX-E36) remained in a GF environment.

Gut microbiota transplantation with cecal content from donor mice fed lard or fish oil for 11 weeks was performed on male 12-week-old mice. Before the microbial transplantation, recipient mice were treated with a 200 μl antibiotic cocktail (ampicillin, 1 g/l; metronidazole, 1 g/l; vancomycin, 0.5 g/l; neomycin, 0.5 g/l) administrated by oral gavage once a day for 3 days. During the last 8 hr of antibiotic treatment, mice were fed either lard or fish oil to facilitate subsequent colonization. Half a frozen cecum was suspended in 5 ml of PBS containing 0.2 g/l Na_2S and 0.5 g/l cysteine as reducing agents in Hungate tubes. Mice were colonized by oral gavage with 200 μl of cecal suspension after a 4-hr fast once a week. After the first microbiota gavage, all mice were fed a lard diet for 3 weeks. All experiments were performed with protocols approved by the University of Gothenburg Animal Studies Committee.

Statistical Analysis

Data are shown as means ± SEM. Statistical comparison of two groups was performed using a Student's t test; comparisons of three or more groups were analyzed by one-way ANOVA with ad hoc Tukey post tests; analysis of datasets containing multiple measurements from each mouse (weight gain, ITT, diet consumption, and feeding efficiency) was performed with a two-way ANOVA for repeated measurements; analysis of interaction was performed with a two-way ANOVA; and analysis of covariance was performed on linear regression. Statistical analysis was performed in GraphPad Prism 6 unless otherwise stated.

Additional experimental procedures are described in the Supplemental Experimental Procedures.

ACCESSION NUMBERS

Microarray data have been uploaded to the Gene Expression Omnibus (GEO) database with accession number GSE70922, and bacterial DNA sequencing data have been uploaded to NCBI as PRJNA289917.

SUPPLEMENTAL INFORMATION

Supplemental Information includes Supplemental Experimental Procedures, seven figures, and four tables and can be found with this article online at http://dx.doi.org/10.1016/j.cmet.2015.07.026.

AUTHOR CONTRIBUTIONS

R.C.: designed, performed, and analyzed experiments. V.T., P.K.D., and P.D.C.: performed and analyzed experiments. F.B.: conceived the project and designed and analyzed experiments. R.C. and F.B. wrote the paper. All authors commented and approved the paper.

ACKNOWLEDGMENTS

We thank Rosie Perkins (Wallenberg Laboratory, University of Gothenburg) for editing the manuscript; Anna Hallén, Gunnel Östergren Lunden, Carina Arvidsson, and Alexandra Ferraro Werling for superb technical assistance; Rozita Akrami for bioinformatics assistance; and NOXXON Pharma for providing mNOX-E36 and revmNOX-E36. We thank Professor Willem de Vos (Wageningen University) for donating *Akkermansia muciniphila*, Professor Jan Borén (Wallenberg Laboratory, University of Gothenburg) for donating *Tlr4*$^{-/-}$ mice, and Professor Carina Mallard (Institute of Neuroscience and Physiology, University of Gothenburg) for donating *Tlr2*$^{-/-}$ mice. This work was supported by the Swedish Research Council, the Swedish Foundation for Strategic Research, the Swedish Diabetes Foundation, the Swedish Heart Lung Foundation, the Torsten Söderbergs and Ragnar Söderbergs Foundations, the Novo Nordisk Foundation, the Knut and Alice Wallenberg Foundation, TORNADO (FP7-KBBE-222720; http://www.fp7tornado.eu/), the EU-funded ETHERPATHS project (FP7-KBBE-222639; http://www.etherpaths.org), and a LUA-ALF grant from Västra Götalandsregionen. The computations were performed on resources provided by Swedish National Infrastructure for Computing (SNIC) through the Uppsala Multidisciplinary Center for Advanced Computational Science (UPPMAX). F.B. is a recipient of a European Research Council (ERC) Consolidator grant (615362 - METABASE). P.D.C. is a research associate at FRS-FNRS (Fonds de la Recherche Scientifique) and recipient of a FRFS-WELBIO under grant (WELBIO-CR-2012S-02R) and an ERC Starting Grant 2013 (ERC, Starting grant 336452-ENIGMO).

Received: January 19, 2015
Revised: May 25, 2015
Accepted: July 27, 2015
Published: August 27, 2015

REFERENCES

Amano, S.U., Cohen, J.L., Vangala, P., Tencerova, M., Nicoloro, S.M., Yawe, J.C., Shen, Y., Czech, M.P., and Aouadi, M. (2014). Local proliferation of macrophages contributes to obesity-associated adipose tissue inflammation. Cell Metab. *19*, 162–171.

Amar, J., Chabo, C., Waget, A., Klopp, P., Vachoux, C., Bermúdez-Humarán, L.G., Smirnova, N., Bergé, M., Sulpice, T., Lahtinen, S., et al. (2011). Intestinal mucosal adherence and translocation of commensal bacteria at the early onset of type 2 diabetes: molecular mechanisms and probiotic treatment. EMBO Mol. Med. *3*, 559–572.

Bäckhed, F., Manchester, J.K., Semenkovich, C.F., and Gordon, J.I. (2007). Mechanisms underlying the resistance to diet-induced obesity in germ-free mice. Proc. Natl. Acad. Sci. USA *104*, 979–984.

Baeck, C., Wehr, A., Karlmark, K.R., Heymann, F., Vucur, M., Gassler, N., Huss, S., Klussmann, S., Eulberg, D., Luedde, T., et al. (2012). Pharmacological inhibition of the chemokine CCL2 (MCP-1) diminishes liver macrophage infiltration and steatohepatitis in chronic hepatic injury. Gut *61*, 416–426.

Björkbacka, H., Kunjathoor, V.V., Moore, K.J., Koehn, S., Ordija, C.M., Lee, M.A., Means, T., Halmen, K., Luster, A.D., Golenbock, D.T., and Freeman, M.W. (2004). Reduced atherosclerosis in MyD88-null mice links elevated serum cholesterol levels to activation of innate immunity signaling pathways. Nat. Med. *10*, 416–421.

Buckley, J.D., and Howe, P.R. (2009). Anti-obesity effects of long-chain omega-3 polyunsaturated fatty acids. Obes. Rev. *10*, 648–659.

Caesar, R., Fåk, F., and Bäckhed, F. (2010). Effects of gut microbiota on obesity and atherosclerosis via modulation of inflammation and lipid metabolism. J. Intern. Med. *268*, 320–328.

Caesar, R., Reigstad, C.S., Bäckhed, H.K., Reinhardt, C., Ketonen, M., Lundén, G.Ö., Cani, P.D., and Bäckhed, F. (2012). Gut-derived lipopolysaccharide augments adipose macrophage accumulation but is not essential for impaired glucose or insulin tolerance in mice. Gut *61*, 1701–1707.

Calder, P.C. (2006). n-3 polyunsaturated fatty acids, inflammation, and inflammatory diseases. Am. J. Clin. Nutr. *83*, 1505S–1519S.

Cani, P.D., Amar, J., Iglesias, M.A., Poggi, M., Knauf, C., Bastelica, D., Neyrinck, A.M., Fava, F., Tuohy, K.M., Chabo, C., et al. (2007). Metabolic endotoxemia initiates obesity and insulin resistance. Diabetes *56*, 1761–1772.

Cinti, S., Mitchell, G., Barbatelli, G., Murano, I., Ceresi, E., Faloia, E., Wang, S., Fortier, M., Greenberg, A.S., and Obin, M.S. (2005). Adipocyte death defines macrophage localization and function in adipose tissue of obese mice and humans. J. Lipid Res. *46*, 2347–2355.

Creely, S.J., McTernan, P.G., Kusminski, C.M., Fisher, M., Da Silva, N.F., Khanolkar, M., Evans, M., Harte, A.L., and Kumar, S. (2007). Lipopolysaccharide activates an innate immune system response in human adipose tissue in obesity and type 2 diabetes. Am. J. Physiol. Endocrinol. Metab. *292*, E740–E747.

David, L.A., Maurice, C.F., Carmody, R.N., Gootenberg, D.B., Button, J.E., Wolfe, B.E., Ling, A.V., Devlin, A.S., Varma, Y., Fischbach, M.A., et al. (2014). Diet rapidly and reproducibly alters the human gut microbiome. Nature *505*, 559–563.

Devkota, S., Wang, Y., Musch, M.W., Leone, V., Fehlner-Peach, H., Nadimpalli, A., Antonopoulos, D.A., Jabri, B., and Chang, E.B. (2012). Dietary-fat-induced taurocholic acid promotes pathobiont expansion and colitis in Il10-/- mice. Nature *487*, 104–108.

Ding, S., Chi, M.M., Scull, B.P., Rigby, R., Schwerbrock, N.M.J., Magness, S., Jobin, C., and Lund, P.K. (2010). High-fat diet: bacteria interactions promote intestinal inflammation which precedes and correlates with obesity and insulin resistance in mouse. PLoS ONE *5*, e12191.

Everard, A., Belzer, C., Geurts, L., Ouwerkerk, J.P., Druart, C., Bindels, L.B., Guiot, Y., Derrien, M., Muccioli, G.G., Delzenne, N.M., et al. (2013). Cross-talk between Akkermansia muciniphila and intestinal epithelium controls diet-induced obesity. Proc. Natl. Acad. Sci. USA *110*, 9066–9071.

Everard, A., Geurts, L., Caesar, R., Van Hul, M., Matamoros, S., Duparc, T., Denis, R.G.P., Cochez, P., Pierard, F., Castel, J., et al. (2014). Intestinal epithelial MyD88 is a sensor switching host metabolism towards obesity according to nutritional status. Nat. Commun. *5*, 5648.

Fleissner, C.K., Huebel, N., Abd El-Bary, M.M., Loh, G., Klaus, S., and Blaut, M. (2010). Absence of intestinal microbiota does not protect mice from diet-induced obesity. Br. J. Nutr. *104*, 919–929.

Guarner, F., Perdigon, G., Corthier, G., Salminen, S., Koletzko, B., and Morelli, L. (2005). Should yoghurt cultures be considered probiotic? Br. J. Nutr. *93*, 783–786.

Henao-Mejia, J., Elinav, E., Jin, C., Hao, L., Mehal, W.Z., Strowig, T., Thaiss, C.A., Kau, A.L., Eisenbarth, S.C., Jurczak, M.J., et al. (2012). Inflammasome-mediated dysbiosis regulates progression of NAFLD and obesity. Nature *482*, 179–185.

Hooper, L.V., Littman, D.R., and Macpherson, A.J. (2012). Interactions between the microbiota and the immune system. Science *336*, 1268–1273.

Hosoi, T., Yokoyama, S., Matsuo, S., Akira, S., and Ozawa, K. (2010). Myeloid differentiation factor 88 (MyD88)-deficiency increases risk of diabetes in mice. PLoS ONE *5*, e12537.

Huang, S., Rutkowsky, J.M., Snodgrass, R.G., Ono-Moore, K.D., Schneider, D.A., Newman, J.W., Adams, S.H., and Hwang, D.H. (2012). Saturated fatty acids activate TLR-mediated proinflammatory signaling pathways. J. Lipid Res. *53*, 2002–2013.

Ivanov, I.I., Atarashi, K., Manel, N., Brodie, E.L., Shima, T., Karaoz, U., Wei, D., Goldfarb, K.C., Santee, C.A., Lynch, S.V., et al. (2009). Induction of intestinal Th17 cells by segmented filamentous bacteria. Cell *139*, 485–498.

Jin, C., and Flavell, R.A. (2013). Innate sensors of pathogen and stress: linking inflammation to obesity. J. Allergy Clin. Immunol. *132*, 287–294.

Kamei, N., Tobe, K., Suzuki, R., Ohsugi, M., Watanabe, T., Kubota, N., Ohtsuka-Kowatari, N., Kumagai, K., Sakamoto, K., Kobayashi, M., et al. (2006). Overexpression of monocyte chemoattractant protein-1 in adipose tissues causes macrophage recruitment and insulin resistance. J. Biol. Chem. *281*, 26602–26614.

Kanda, H., Tateya, S., Tamori, Y., Kotani, K., Hiasa, K., Kitazawa, R., Kitazawa, S., Miyachi, H., Maeda, S., Egashira, K., and Kasuga, M. (2006). MCP-1 contributes to macrophage infiltration into adipose tissue, insulin resistance, and hepatic steatosis in obesity. J. Clin. Invest. *116*, 1494–1505.

Kennedy, A., Martinez, K., Chuang, C.-C., LaPoint, K., and McIntosh, M. (2009). Saturated fatty acid-mediated inflammation and insulin resistance in adipose tissue: mechanisms of action and implications. J. Nutr. *139*, 1–4.

Kim, J.J., and Sears, D.D. (2010). TLR4 and insulin resistance. Gastroenterol. Res. Pract. *2010*, 11.

Kopp, A., Buechler, C., Neumeier, M., Weigert, J., Aslanidis, C., Schölmerich, J., and Schäffler, A. (2009). Innate immunity and adipocyte function: ligand-specific activation of multiple Toll-like receptors modulates cytokine, adipokine, and chemokine secretion in adipocytes. Obesity (Silver Spring) *17*, 648–656.

Kriegel, M.A., Sefik, E., Hill, J.A., Wu, H.-J., Benoist, C., and Mathis, D. (2011). Naturally transmitted segmented filamentous bacteria segregate with diabetes protection in nonobese diabetic mice. Proc. Natl. Acad. Sci. USA *108*, 11548–11553.

Kulkarni, O., Pawar, R.D., Purschke, W., Eulberg, D., Selve, N., Buchner, K., Ninichuk, V., Segerer, S., Vielhauer, V., Klussmann, S., and Anders, H.J. (2007). Spiegelmer inhibition of CCL2/MCP-1 ameliorates lupus nephritis in MRL-(Fas)lpr mice. J. Am. Soc. Nephrol. *18*, 2350–2358.

Kulkarni, O., Eulberg, D., Selve, N., Zöllner, S., Allam, R., Pawar, R.D., Pfeiffer, S., Segerer, S., Klussmann, S., and Anders, H.J. (2009). Anti-Ccl2 Spiegelmer permits 75% dose reduction of cyclophosphamide to control diffuse proliferative lupus nephritis and pneumonitis in MRL-Fas(lpr) mice. J. Pharmacol. Exp. Ther. *328*, 371–377.

Larsson, E., Tremaroli, V., Lee, Y.S., Koren, O., Nookaew, I., Fricker, A., Nielsen, J., Ley, R.E., and Bäckhed, F. (2012). Analysis of gut microbial regulation of host gene expression along the length of the gut and regulation of gut microbial ecology through MyD88. Gut *61*, 1124–1131.

Lee, B.-C., and Lee, J. (2014). Cellular and molecular players in adipose tissue inflammation in the development of obesity-induced insulin resistance. Biochim. Biophys. Acta *1842*, 446–462.

Michelsen, K.S., Wong, M.H., Shah, P.K., Zhang, W., Yano, J., Doherty, T.M., Akira, S., Rajavashisth, T.B., and Arditi, M. (2004). Lack of Toll-like receptor 4 or myeloid differentiation factor 88 reduces atherosclerosis and alters plaque phenotype in mice deficient in apolipoprotein E. Proc. Natl. Acad. Sci. USA *101*, 10679–10684.

Oh, D.Y., Talukdar, S., Bae, E.J., Imamura, T., Morinaga, H., Fan, W., Li, P., Lu, W.J., Watkins, S.M., and Olefsky, J.M. (2010). GPR120 is an omega-3 fatty acid receptor mediating potent anti-inflammatory and insulin-sensitizing effects. Cell *142*, 687–698.

Rabot, S., Membrez, M., Bruneau, A., Gérard, P., Harach, T., Moser, M., Raymond, F., Mansourian, R., and Chou, C.J. (2010). Germ-free C57BL/6J mice are resistant to high-fat-diet-induced insulin resistance and have altered cholesterol metabolism. FASEB J. *24*, 4948–4959.

Richards, M.R., Black, A.S., Bonnet, D.J., Barish, G.D., Woo, C.W., Tabas, I., Curtiss, L.K., and Tobias, P.S. (2013). The LPS2 mutation in TRIF is atheroprotective in hyperlipidemic low density lipoprotein receptor knockout mice. Innate Immun. *19*, 20–29.

Scott, K.P., Gratz, S.W., Sheridan, P.O., Flint, H.J., and Duncan, S.H. (2013). The influence of diet on the gut microbiota. Pharmacol. Res. *69*, 52–60.

Shi, H., Kokoeva, M.V., Inouye, K., Tzameli, I., Yin, H., and Flier, J.S. (2006). TLR4 links innate immunity and fatty acid-induced insulin resistance. J. Clin. Invest. *116*, 3015–3025.

Shin, N.-R., Lee, J.-C., Lee, H.-Y., Kim, M.-S., Whon, T.W., Lee, M.-S., and Bae, J.-W. (2014). An increase in the Akkermansia spp. population induced by metformin treatment improves glucose homeostasis in diet-induced obese mice. Gut *63*, 727–735.

Tremaroli, V., and Bäckhed, F. (2012). Functional interactions between the gut microbiota and host metabolism. Nature *489*, 242–249.

Velagapudi, V.R., Hezaveh, R., Reigstad, C.S., Gopalacharyulu, P., Yetukuri, L., Islam, S., Felin, J., Perkins, R., Borén, J., Orešič, M., and Bäckhed, F. (2010). The gut microbiota modulates host energy and lipid metabolism in mice. J. Lipid Res. *51*, 1101–1112.

Weisberg, S.P., McCann, D., Desai, M., Rosenbaum, M., Leibel, R.L., and Ferrante, A.W., Jr. (2003). Obesity is associated with macrophage accumulation in adipose tissue. J. Clin. Invest. *112*, 1796–1808.

Weisberg, S.P., Hunter, D., Huber, R., Lemieux, J., Slaymaker, S., Vaddi, K., Charo, I., Leibel, R.L., and Ferrante, A.W., Jr. (2006). CCR2 modulates inflammatory and metabolic effects of high-fat feeding. J. Clin. Invest. *116*, 115–124.

Wlotzka, B., Leva, S., Eschgfäller, B., Burmeister, J., Kleinjung, F., Kaduk, C., Muhn, P., Hess-Stumpp, H., and Klussmann, S. (2002). In vivo properties of an anti-GnRH Spiegelmer: an example of an oligonucleotide-based therapeutic substance class. Proc. Natl. Acad. Sci. USA *99*, 8898–8902.

Yu, L., Wang, L., and Chen, S. (2010). Endogenous toll-like receptor ligands and their biological significance. J. Cell. Mol. Med. *14*, 2592–2603.

Cell Metabolism, Volume *22*

Supplemental Information

Crosstalk between Gut Microbiota and Dietary Lipids Aggravates WAT Inflammation through TLR Signaling

Robert Caesar, Valentina Tremaroli, Petia Kovatcheva-Datchary, Patrice D. Cani, and Fredrik Bäckhed

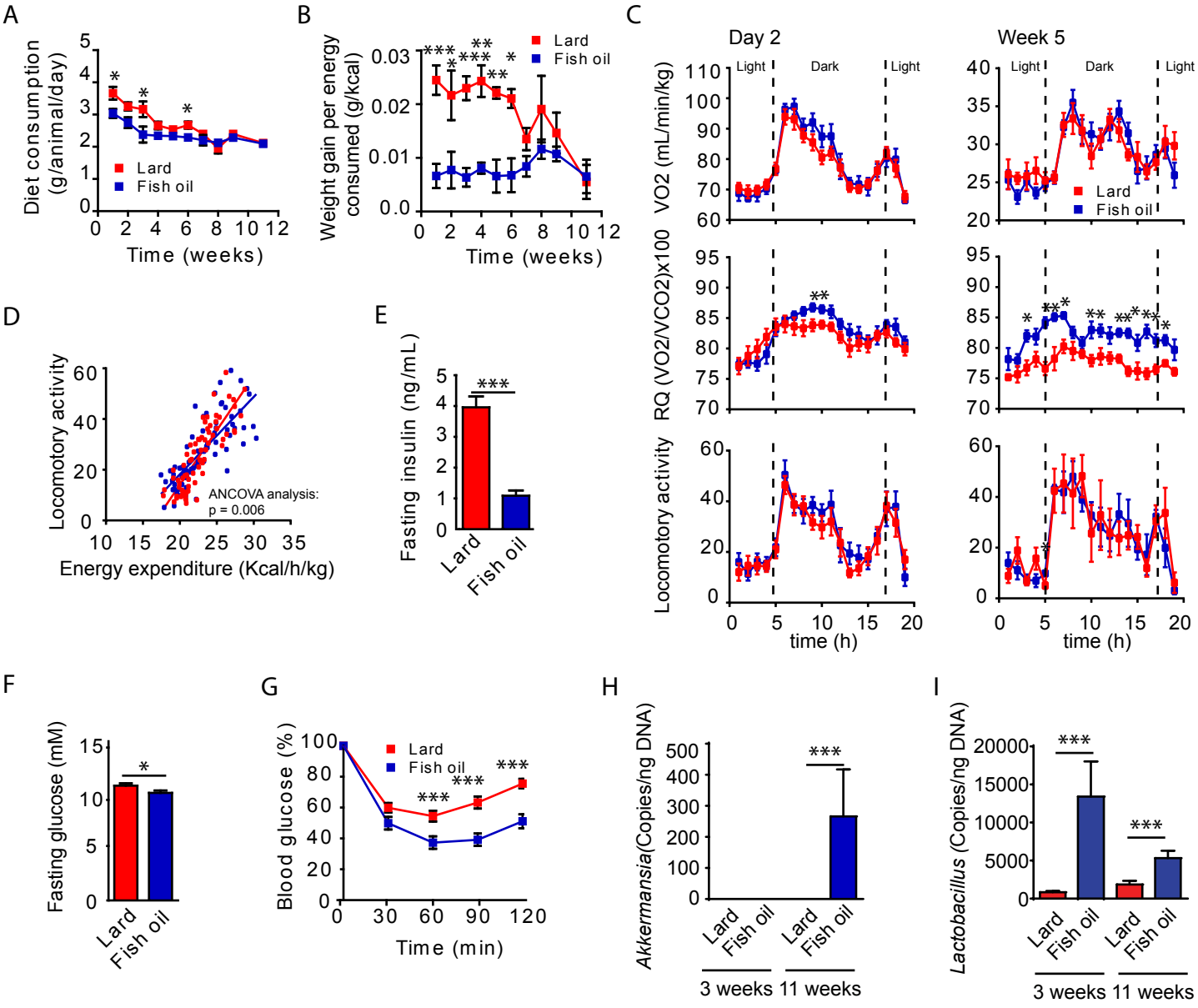

Supplementary Figure 1. Energy balance and glucose homeostasis in mice fed lard or fish oil. Related to Figure 1. (A) Food consumption during high-fat diet (n=3-4 cages/time-point). (B) Efficiency of feeding measured as gram body weight gained per kcal consumed (n=3-4 cages/time-point). (C) VO2 consumption, respiratory quotient (RQ) and locomotory activity measured over 18 h, including two light and one dark periods, in mice fed lard or fish oil for 2 days of for 5 weeks. Measurements performed on single-caged mice using SOMEDIC metabolic systems and G2 E-Mitter telemetry devices [n=8 (2 days); 5 (5 weeks)]. (D) Correlation analysis between energy expenditure and locomotory activity in mice fed lard or fish oil for 2 days. Correlation between locomotory activity and energy expenditure was based on average values collected over 18 h. Each dot represents data collected in 2 h intervals. 8 mice were used for each dietary group resulting in a total of 72 data points for each dietary group. Energy expenditure was calculated by the equation (3.815 + 1.232*RQ)×VO2. ANCOVA analysis was performed to determine difference in slope between linear regression lines. Fasting (E) insulin and (F) glucose levels in mice fed lard or fish oil for 11 weeks (n=9-10 mice per group). (G) Insulin tolerance in mice fed lard or fish oil (n=9-10 mice per group) for 10 weeks. Abundance of (H) *Akkermansia* and (I) *Lactobacillus* in cecum of mice fed lard or fish oil for 3 weeks (N=9 mice per group) and 11 weeks (N=15 mice per group). Quantification of bacteria was performed by qPCR.

Mean values ± SEM are plotted; *p<0.05, **p<0.01, ***p<0.001 versus fish oil.

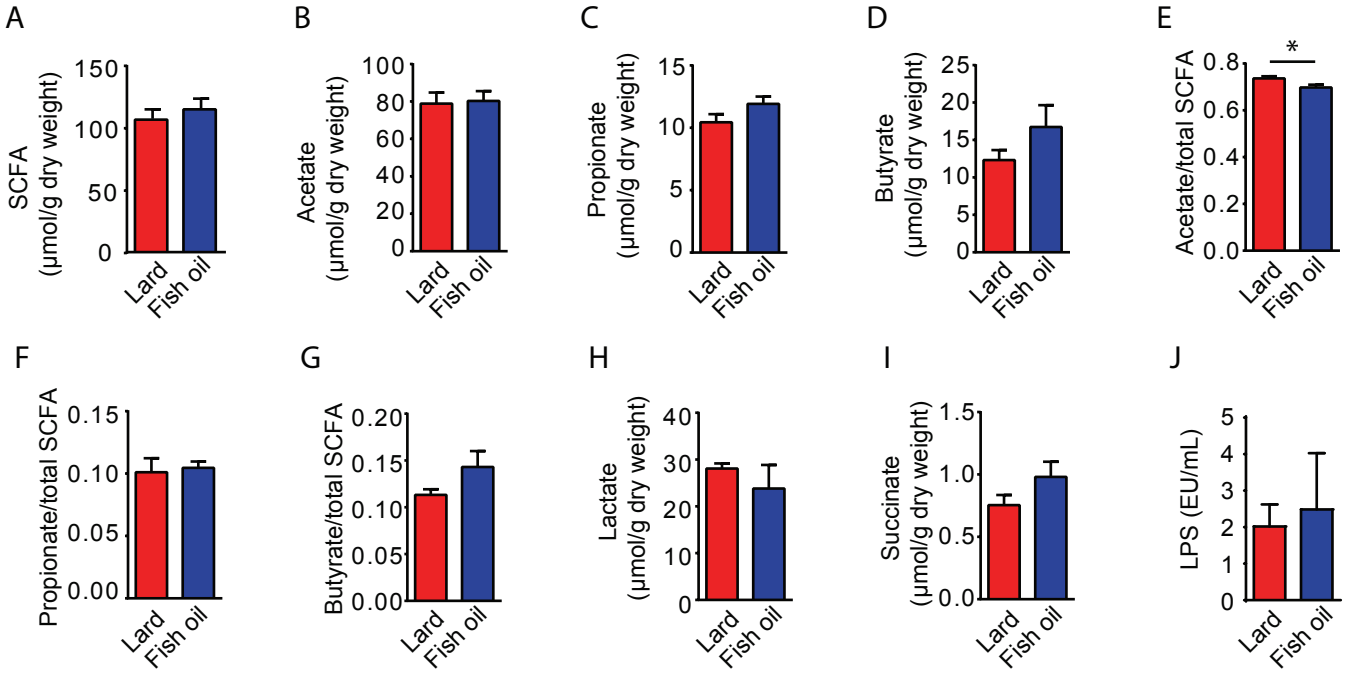

Supplementary Figure 2. Abundance of SCFA in mice fed lard or fish oil. Related to Figure 1.
Abundance of (A) total SCFA, (B) acetate, (C) propionate and (D) butyrate in cecum of mice fed lard diet or fish oil for 11 weeks (n=6 mice per group. Ratios between (E) acetate, (F) propionate and (G) butyrate and total abundance of SCFA (based on data presented in panels A-D). Abundance of (H) lactate and (I) succinate in cecum of mice fed lard or fish oil for 11 weeks. (J) Abundance of LPS in serum from mice fed lard or fish oil for 3 weeks (n=7-8 mice per group).
Mean values ± SEM are plotted; *$p<0.05$.

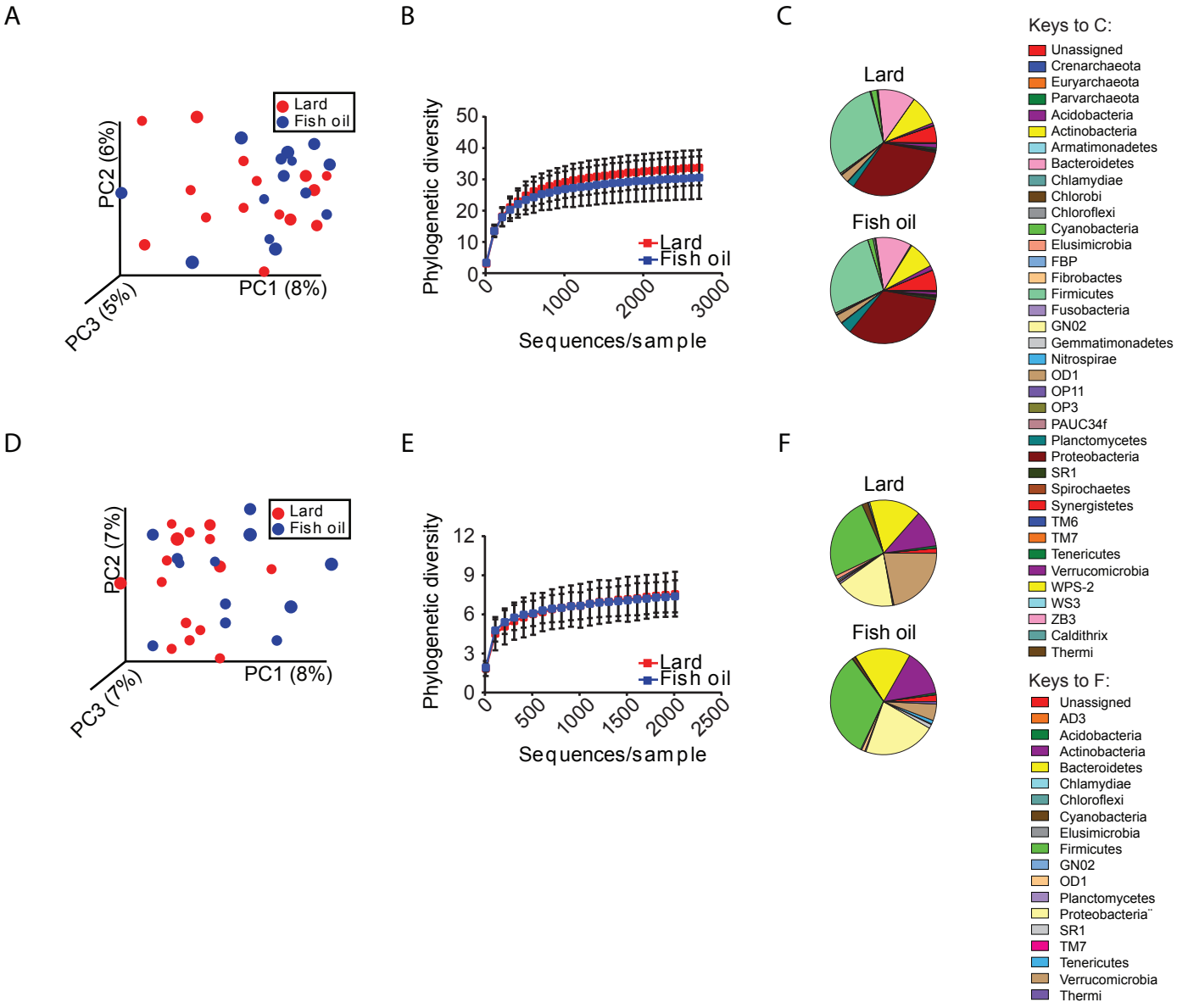

Supplementary Figure 3. Microbiota in blood and epididymal WAT of mice fed lard or fish oil for 11 weeks. Related to Figure 2.

(A) Principal coordinate analysis of blood microbiota composition based on unweighted UniFrac in mice fed lard or fish oil [n=14 (lard), n=15 (fish oil)]; no amplification product with 515F and 806R primers could be obtained for one lard blood sample). (B) Rarefaction curves for phylogenetic diversity in blood microbiota from mice fed lard or fish oil (10-2710 sequences/sample). (C) Pie charts of blood microbial phyla composition in mice fed lard or fish oil for 11 weeks. (D) Principal coordinate analysis of WAT microbiota composition based on unweighted UniFrac in mice fed lard or fish oil [n=12 (lard), n=15 (fish oil)]; the depth of sequencing for three lard WAT samples was lower than 2000 sequences/samples so these samples were excluded from microbiota analyses). (E) Rarefaction curves for phylogenetic diversity in WAT microbiota from mice fed lard or fish oil (10-2010 sequences/sample). (F) Pie charts of WAT microbial phyla composition in mice fed lard or fish oil for 11 weeks.

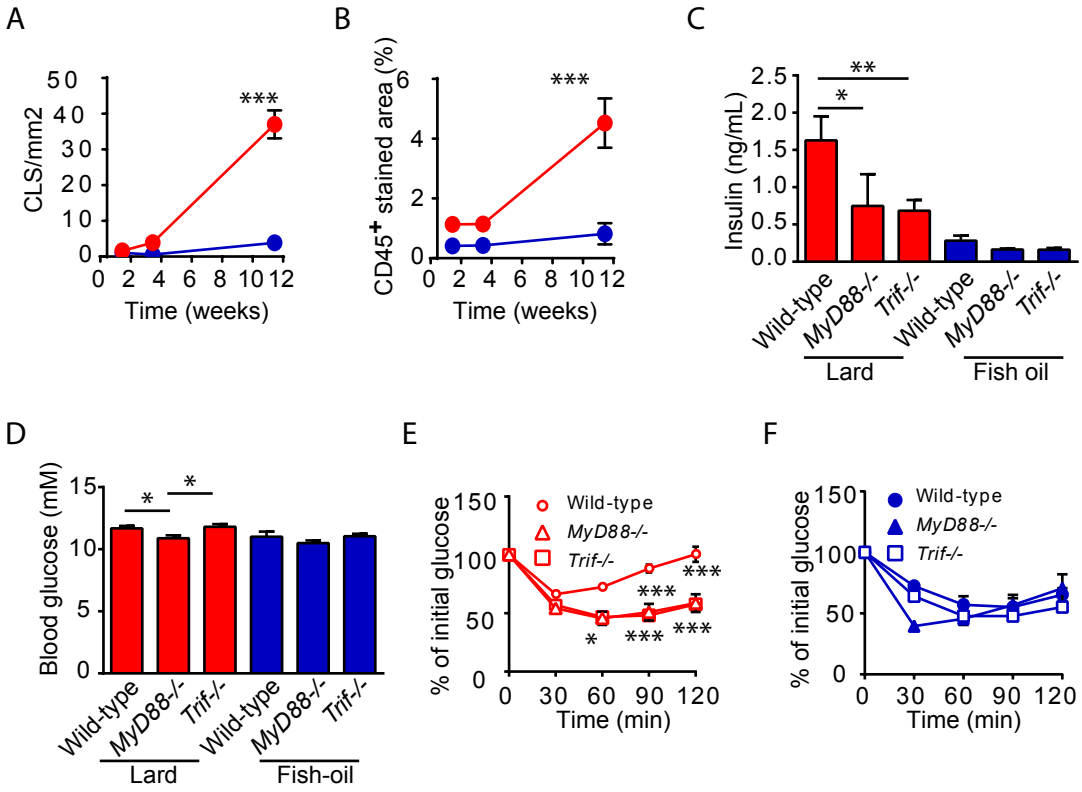

Supplementary Figure 4. WAT inflammation in wild-type mice after 1, 3 and 11 weeks of lard or fish oil diet and glucose homeostasis in wild-type, *Myd88-/-* and *Trif-/-* mice after 10 weeks of lard or fish oil diet. Related to Figure 3. (A) Quantification of crown-like structures in wild-type mice fed lard or fish-oil for 1, 3 or 11 weeks [n=10 (wild-type lard 1 week); 10 (wild-type lard 3 week); 7 (wild-type lard 11 week); 10 (wild-type fish oil 1 week); 10 (wild-type fish oil 3 weeks); 7 (wild-type fish oil 11 week)]. (B) Percentage of area occupied by $CD45^+$ cells in WAT from wild-type mice fed lard or fish-oil for 1, 3 or 11 weeks [n=10 (wild-type lard 1 week); 10 (wild-type lard 3 week); 7 (wild-type lard 11 week); 10 (wild-type fish oil 1 week); 10 (wild-type fish oil 3 weeks); 7 (wild-type fish oil 11 week)]. Fasting (C) insulin and (D) glucose levels in mice fed lard or fish oil for 11 weeks [n=6 (wild-type lard); 4 (*Myd88-/-* lard); 6 (*Trif-/-* lard); 3 (wild-type fish oil); 9 (*Myd88-/-* fish oil); 9 (*Trif-/-* fish oil)]. Insulin tolerance in mice fed (E) lard [n=3 (wild-type); 7 (*Myd88-/-*); 8 (*Trif-/-*)] or (F) fish oil [(n=3 (wild-type); 4 (*Myd88-/-*); 6 (*Trif-/-*)] for 10 weeks.
Mean values ±SEM are plotted; *p<0.05, **p<0.01, ***p<0.001.

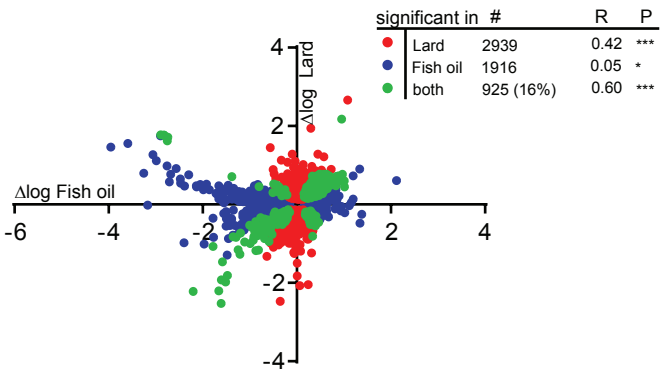

Supplementary Figure 5. Gene regulation by the gut microbiota in mice fed lard or fish oil. Related to Figure 4. Regulation of WAT genes induced by the gut microbiota in mice fed lard (y-axis) or fish oil (x-axis). Genes significantly regulated ($p<0.05$, corrected for FDR) are displayed. The embedded table displays the number of regulated genes unique to either of the dietary groups or common to both and the R-value and p-value associated with a linear regression analysis of the dataset (n=6 mice).
Mean values ± SEM are plotted; *$p<0.05$, ***$p<0.001$.

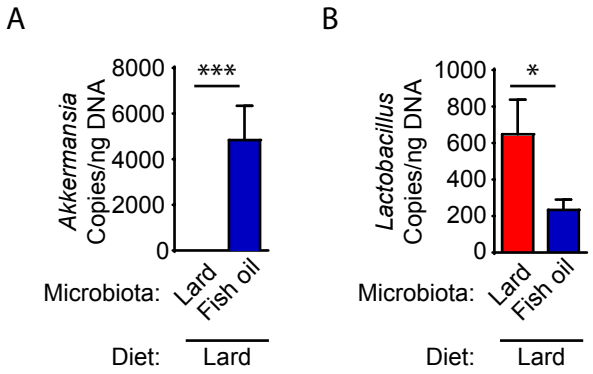

Supplementary Figure 6. . Abundance of bacterial taxa in mice transplanted with cecal microbiota from donor mice fed lard or fish oil for 11 weeks. Related to Figure 5. (A-C) Abundance of *Akkermansia* and *Lactobacillus* in cecum of mice fed lard for 3 weeks and transplanted with cecal microbiota from donor mice fed lard or fish oil for 11 weeks (n=10 mice per group). Quantification of bacteria was performed by qPCR.
Mean values ±SEM are plotted; *p<0.05, ***p<0.001.

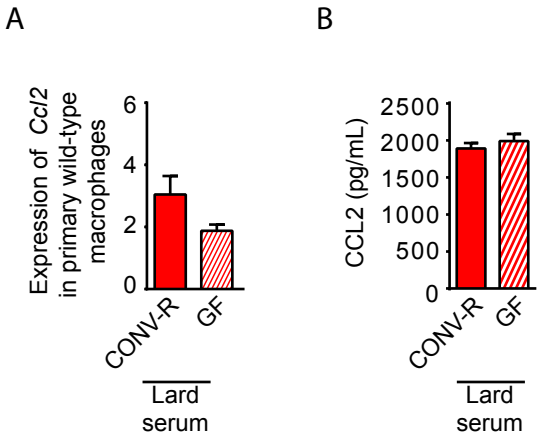

Supplementary Figure 7. Expression and secretion of CCL2 in primary macrophages. Related to Figure 6. (A) Expression of *Ccl2* and (B) CCL2 secretion in primary wild-type macrophages stimulated for 4 h with 2% plasma isolated from *vena cava* of CONV-R and GF mice fed lard (n=5-6 mice per group). Mean values ± SEM are plotted.

Supplementary Table 1. Diet composition. Related to Figure 1.

	D10011202 (lard diet)		D05122102 (Fish-oil diet)	
	g (%)	**kcal (%)**	**g (%)**	**kcal (%)**
Protein	24	20	24	20
Carbohydrate	41	35	41	35
Fat	23	45	23	45
Total		100		100
	kcal/g		**kcal/g**	
	4.72		4.73	
	g/unit	**kcal/unit**	**g/unit**	**kcal/unit**
Casein, 80 Mesh	200	800	200	800
L-Cysteine	3	12	3	12
Corn Starch	72.8	291	72.8	291
Maltodextrin 10	100	400	100	400
Sucrose	172.8	691	172.8	691
Cellulose	50		50	
Soybean oil	25	225	25	225
Lard	177.7	1598		
Menhaden Oil			177.7	1598
tert-Butylhydroquinone	0.0355			
Mineral Mix S10026	10		10	
DiCalcium Phosphate	13		13	
Calcium Carbonate	5.5		5.5	
Potassium Citrate	16.5		16.5	
Vitamin mix V10001	10	40	10	40
Choline Bitartrate	2		2	
Cholesterol	0.54			
Total	858.73	4057	858.15	4057
Cholesterol (g)	0.709		0.71	
Cholesterol (%)	0.083		0.083	
tBHQ (g)	0.035		0.035	

Supplementary Table 2. Relative abundance of phyla and of genera differentially abundant in gut microbiota from mice fed lard or fish oil for 11 weeks (p<0.05, FDR correction for multiple testing). Related to Figure 1.

		Relative abundance		Fold change
Phylum	**FDR**	**Lard**	**Fish oil**	**(Lard/Fish oil)**
Bacteroidetes	0.038	2.30E-01	1.46E-01	1.57
Unassigned;Other	0.31	4.18E-03	2.74E-03	1.53
Deferribacteres	0.32	2.72E-02	1.82E-02	1.49
Verrucomicrobia	0.026	4.59E-04	1.42E-03	0.32
TM7	0.026	1.15E-04	4.93E-04	0.23
Proteobacteria	0.038	5.11E-02	9.97E-02	0.51
Tenericutes	0.13	3.44E-04	6.07E-04	0.57
Actinobacteria	0.32	7.74E-03	8.82E-03	0.88
Cyanobacteria	0.32	1.67E-04	3.22E-04	0.52
Bacteria;Other	0.55	2.15E-03	2.42E-03	0.89
Firmicutes	0.78	6.77E-01	7.19E-01	0.94
Taxon				
p_Proteobacteria|c_Deltaproteobacteria|o_Desulfovibrionales|f_Desulfovibrionaceae|g_Bilophila	0.042	4.44E-03	1.14E-04	39.05
p_Bacteroidetes|c_Bacteroidia|o_Bacteroidales|f_|g_	0.012	9.12E-03	1.57E-03	5.79
p_Bacteroidetes|c_Bacteroidia|o_Bacteroidales|f_Bacteroidaceae|g_Bacteroides	0.038	1.31E-01	4.41E-02	2.98
p_Firmicutes|c_Clostridia|o_Clostridiales|f_Lachnospiraceae|Other	0.040	3.71E-02	2.10E-02	1.77
p_Firmicutes|c_Clostridia|o_Clostridiales|f_Ruminococcaceae|g_Ruminococcus	0.040	1.74E-02	1.02E-02	1.70
p_Bacteroidetes|c_Bacteroidia|o_Bacteroidales|f_S24-7|g_	0.041	5.26E-02	8.37E-02	0.63
p_Proteobacteria|c_Deltaproteobacteria|o_Desulfovibrionales|f_Desulfovibrionaceae|g_	0.041	4.57E-02	9.82E-02	0.47
p_Firmicutes|c_Bacilli|o_Lactobacillales|f_Streptococcaceae|g_Streptococcus	0.042	1.36E-04	3.98E-04	0.34
p_Verrucomicrobia|c_Verrucomicrobiae|o_Verrucomicrobiales|f_Verrucomicrobiaceae|g_Akkermansia	0.037	4.59E-04	1.42E-03	0.32
p_Firmicutes|c_Clostridia|o_Clostridiales|f_Lachnospiraceae|g_Coprococcus	0.012	6.63E-03	2.83E-02	0.23
p_TM7|c_TM7-3|o_CW040|f_F16|g_	0.038	1.15E-04	4.93E-04	0.23
p_Firmicutes|c_Bacilli|o_Lactobacillales|f_Lactobacillaceae|g_Lactobacillus	0.012	4.79E-03	2.39E-02	0.20
p_Firmicutes|c_Clostridia|o_Clostridiales|f_Clostridiaceae|g_Candidatus Arthromitus	0.040	0.00E+00	2.28E-04	0.00
p_Firmicutes|c_Clostridia|o_Clostridiales|f_Peptococcaceae|g_rc4-4	0.040	0.00E+00	1.19E-03	0.00

Supplementary Table 3. Functional analysis of gene regulation induced by diet (lard or fish oil for 11 weeks) in WAT. Related to Figure 4 and Supplementary Figure 5.

GO term	Description	Bonferroni
Categories enriched in WAT of mice fed lard		
278	mitotic cell cycle	$4.2x10^{-15}$
51301	cell division	$2.1x10^{-13}$
45321	leukocyte activation	$4.2x10^{-13}$
1775	cell activation	$1.7x10^{-12}$
48285	organelle fission	$5.8x10^{-12}$
35556	intracellular signal transduction	$2.6x10^{-08}$
1817	regulation of cytokine production	$1.4x10^{-07}$
30029	actin filament-based process	$1.8x10^{-06}$
6954	inflammatory response	$5.5x10^{-06}$
9611	response to wounding	$7.6x10^{-06}$
6260	DNA replication	$1.6x10^{-05}$
7059	chromosome segregation	$4.3x10^{-05}$
6793	phosphorus metabolic process	$4.6x10^{-05}$
6796	phosphate-containing compound metabolic process	$4.6x10^{-05}$
6897	endocytosis	$1.9x10^{-04}$
10324	membrane invagination	$1.9x10^{-04}$
6935	chemotaxis	$3.7x10^{-04}$
6259	DNA metabolic process	$3.9x10^{-04}$
6468	protein phosphorylation	$4.1x10^{-04}$
44093	positive regulation of molecular function	$1.3x10^{-03}$
32943	mononuclear cell proliferation	$2.7x10^{-03}$
8219	cell death	$1.2x10^{-02}$
16265	death	$2.1x10^{-02}$
7017	microtubule-based process	$2.2x10^{-02}$
42325	regulation of phosphorylation	$2.5x10^{-02}$
6665	sphingolipid metabolic process	$3.0x10^{-02}$
51174	regulation of phosphorus metabolic process	$4.6x10^{-02}$
Categories enriched in WAT of mice fed fish oil		
6091	generation of precursor metabolites and energy	$4.7x10^{-32}$
22900	electron transport chain	$3.4x10^{-24}$
6412	translation	$1.2x10^{-20}$
55114	oxidation-reduction process	$6.0x10^{-19}$
6732	coenzyme metabolic process	$4.6x10^{-10}$
51186	cofactor metabolic process	$3.1x10^{-08}$
19318	hexose metabolic process	$1.6x10^{-04}$
6631	fatty acid metabolic process	$9.2x10^{-04}$
7005	mitochondrion organization	$1.8x10^{-03}$
9081	branched-chain amino acid metabolic process	$4.1x10^{-02}$

Supplementary Table 4. Functional analysis of gene regulation induced by gut microbiota or interaction between gut microbiota and diet in WAT from mice fed lard or fish oil for 11 weeks. Related to Figure 4 and Supplementary Figure 5.

GO term	Description	Bonferroni
Categories enriched in genes increased by gut microbiota in WAT of mice fed lard		
6396	RNA processing	$1.8x10^{-12}$
6397	mRNA processing	$1.1x10^{-11}$
16071	mRNA metabolic process	$1.1x10^{-09}$
6091	generation of precursor metabolites and energy	$1.4x10^{-04}$
6457	protein folding	$1.6x10^{-04}$
22900	electron transport chain	$2.4x10^{-04}$
7005	mitochondrion organization	$1.5x10^{-03}$
44265	cellular macromolecule catabolic process	$8.3x10^{-03}$
22613	ribonucleoprotein complex biogenesis	$9.6x10^{-03}$
9057	macromolecule catabolic process	$1.2x10^{-02}$
2504	antigen processing and presentation of antigen MHC class II	$1.2x10^{-02}$
Categories enriched in genes reduced by gut microbiota in WAT of mice fed lard		
6091	generation of precursor metabolites and energy	$4.7x10^{-32}$
22900	electron transport chain	$3.4x10^{-24}$
6412	translation	$1.2x10^{-20}$
55114	oxidation-reduction process	$6.0x10^{-19}$
6732	coenzyme metabolic process	$4.6x10^{-10}$
51186	cofactor metabolic process	$3.1x10^{-08}$
19318	hexose metabolic process	$1.6x10^{-04}$
6631	fatty acid metabolic process	$9.2x10^{-04}$
7005	mitochondrion organization	$1.8x10^{-03}$
9081	branched-chain amino acid metabolic process	$4.1x10^{-02}$
Categories enriched in genes induced by gut microbiota in WAT of mice fed fish oil		
6412	translation	$1.9x10^{-42}$
6091	generation of precursor metabolites and energy	$4.4x10^{-38}$
22900	electron transport chain	$5.9x10^{-33}$
55114	oxidation-reduction process	$3.1x10^{-19}$
34660	ncRNA metabolic process	$3.3x10^{-12}$
7005	mitochondrion organization	$5.7x10^{-10}$
6399	tRNA metabolic process	$9.5x10^{-09}$
6396	RNA processing	$3.5x10^{-08}$
51186	cofactor metabolic process	$1.3x10^{-07}$
22613	ribonucleoprotein complex biogenesis	$5.2x10^{-07}$
34613	cellular protein localization	$1.5x10^{-05}$
6732	coenzyme metabolic process	$1.1x10^{-04}$
6413	translational initiation	$2.3x10^{-03}$
8610	lipid biosynthetic process	$3.2x10^{-03}$
Categories enriched in genes reduced by gut microbiota in WAT of mice fed fish oil		
9611	response to wounding	$1.1x10^{-11}$
51056	regulation of GTPase mediated signal transduction	$8.1x10^{-08}$
6954	inflammatory response	$8.7x10^{-06}$
50817	coagulation	$3.9x10^{-04}$
2252	immune effector process	$1.6x10^{-03}$
1775	cell activation	$7.5x10^{-03}$
6897	endocytosis	$1.1x10^{-02}$
Categories enriched in genes regulated by gut microbiota-diet interaction in Q1(Figure 3H)		
0009611	response to wounding	$1.4x10^{-11}$
0002526	acute inflammatory response	$6.9x10^{-08}$
0006955	immune response	$8.5x10^{-05}$
0050817	coagulation	$1.6x10^{-04}$
0009074	aromatic amino acid family catabolic process	$1.8x10^{-03}$
0055114	oxidation-reduction process	$1.9x10^{-03}$
0048584	positive regulation of response to stimulus	$6.2x10^{-03}$
0019439	aromatic compound catabolic process	$1.1x10^{-02}$
Categories enriched in genes regulated by gut microbiota-diet interaction in Q3 (Figure 3H)		
0015031	protein transport	$1.5x10^{-04}$
0051186	cofactor metabolic process	$1.5x10^{-04}$
0051188	cofactor biosynthetic process	$2.4x10^{-03}$
0006511	ubiquitin-dependent protein catabolic process	$1.0x10^{-02}$

Supplementary Experimental procedures

Telemetry, energy expenditure and food consumption measurements

Telemetry devices (G2 E-Mitter, Mini Mitter, Bend, OR) were implanted in mice two weeks before the experiment according to the surgery protocol provided by the manufacturer. Measurements were performed after 2 days or after 5 weeks of high-fat diet. Only one measurement was performed on each mouse. Oxygen consumption (VO2) and carbon dioxide production (VCO2) were recorded every 2 min for 23 h by indirect calorimetry with a SOMEDIC metabolic system (INCA®, Somedic Sales, Hörby, Sweden), which is built around a sealed chamber and ventilated with a constant flow of air. Animals had *ad libitum* access to food and water during the measurements and the temperature was set to 21°C. The indirect calorimeter was combined with the Mini Mitter telemetry system to measure locomotory activity, defined as the number of changes in direction per minute, and body temperature. The data for the first 3 h were discarded to allow for animal acclimatization to the testing conditions. The respiratory quotient (RQ) was calculated per hour as the VCO2/VO2 ratio. In all calculations, W0.75 was used to correct for body size, according to Kleiber's law (Kleiber, 1932). Energy expenditure was calculated by the equation (3.815 + 1.232*RQ)×VO2.

Insulin tolerance tests and measurements of plasma insulin levels

Insulin tolerance tests were performed after 10 weeks of high-fat diet by intraperitoneal injection of insulin (0.75 U/kg body weight in lard vs. fish-oil diet; 0.375 U/kg in wild-type vs. mutant mice), after a 4 h fast. Tail blood was collected at 0, 30, 60, 90 and 120 min after injection. Blood glucose levels were determined using a HemoCue glucose 201+ analyzer (HemoCue, Ängelholm, Sweden). Insulin was measured with a kit from Crystal Chem (Downers Grove, IL) according to the manufacturer’s protocol.

Extraction of Genomic DNA and Profiling of the 16S rRNA gene by Next Generation sequencing

Total genomic DNA was isolated from 60-100 mg of cecal content, 100 mg of WAT and 50 µl of frozen whole blood collected from the cava vein by using a repeated bead beating method as previously described (Salonen et al., 2010).

The cecal microbiota of mice fed lard or fish oil diets for 11 weeks was sequenced by 454 pyrosequencing of the 16 rRNA gene in the V1-V2 region, amplified with the 27F and barcoded 338R primers fused with sequencing adapters (Hamady et al., 2008). Samples were sequenced in a 454 GS FLX system with Titanium chemistry by GATC Biotech (Konstanz, Germany). Each sample was amplified in triplicate in reaction volumes of 25 µl containing 1.5 U of FastStart Taq DNA Polymerase (Roche), 200 nM of each primer and 20 ng of genomic DNA. PCR was carried out under the following conditions: initial denaturation for 3 min at 95°C, followed by 25 cycles of denaturation for 20 sec at 95°C, annealing for 20 sec at 52°C and elongation for 60 sec at 72°C, and a final elongation step for 8 min at 72°C.

The bacterial DNA present in WAT and blood samples of mice fed lard ad fish oil diets for 11 weeks, and the cecal microbiota of the transplanted mice were profiled by sequencing of the V4 region of the 16S rRNA gene on an Illumina MiSeq (llumina RTA v1.17.28; MCS v2.5) using 515F and 806R primers designed for dual indexing (Kozich et al., 2013) and the V2 kit (2x250 bp paired-end reads). Each sample was amplified in duplicate in reaction volumes of 25 µl containing 1x Five Prime Hot Master Mix (5 PRIME GmbH), 200 nM of each primer, 0.4 mg/ml BSA, 5% DMSO and 20 ng (cecal samples) or 100 ng (WAT and blood samples) of genomic DNA. PCR was carried out under the following conditions: initial denaturation for 3 min at 94°C, followed by 25 cycles (cecal samples) or 35 cycles (blood and WAT samples) of denaturation for 45 sec at 94°C, annealing for 60 sec at 52°C and elongation for 90 sec at 72°C, and a final elongation step for 10 min at 72°C.

Replicates were combined, purified with the NucleoSpin Gel and PCR Clean-up kit (Macherey-Nagel, Germany) and quantified using the Quant-iT PicoGreen dsDNA kit (Invitrogen, Carlsbad, CA). Purified PCR products were diluted to 20 ng/µl and pooled in equal amounts. The pooled amplicons were purified again using Ampure magnetic purification beads (Agencourt, Danvers, MA) to remove short amplification products.

Raw pyrosequencing data was trimmed of the 454 adapter and barcodes, and filtered to remove sequences that were shorter than 200 nucleotides, longer than 1000 nucleotides, contained primer mismatches, ambiguous bases, uncorrectable barcodes, and homopolymer runs in excess of six bases.

Illumina paired-end reads were merged using PEAR (Zhang et al., 2014) and quality filtered with FASTX (Phred score $\geq$ 20 for 100% of the bases in a sequence). For WAT and blood samples sequences that were shorter than 200 nucleotides or longer than 400 were removed from the analysis.

Quality filtered 454 pyrosequencing and Illumina reads were analyzed with the software package QIIME (Caporaso et al., 2010) (version 1.8.0). Sequences were clustered into operational taxonomic units (OTUs) at a 97% identity threshold using an open-reference OTU picking approach with UCLUST (Edgar, 2010) against the Greengenes reference database (DeSantis et al., 2006) (13_8 release). All sequences that failed to cluster when tested against the Greengenes database were used as input for picking OTUs *de novo*. Representative sequences for the OTUs were Greengenes reference sequences or cluster seeds, and were taxonomically assigned using the Greengenes taxonomy and the Ribosomal Database Project Classifier (Wang et al., 2007). Representative OTUs were aligned using PyNAST (Caporaso et al., 2010) and used to build a phylogenetic tree with FastTree (Price et al., 2010), which was used to estimate α- and β-diversity of samples using phylogenetic diversity (Faith, 1992) and unweighted unifrac (Lozupone and Knight, 2005). Three-dimensional principal

coordinates analysis plots were visualized using Emperor (Vázquez-Baeza et al., 2013). Chimeric sequences were identified with ChimeraSlayer (Haas et al., 2011) and excluded from all downstream analyses. Similarly, sequences that could not be aligned with PyNAST, singletons and very low abundant sequences (relative abundance <0.005%) were also excluded.

To correct for differences in sequencing depth, the same amount of sequences was randomly sub-sampled for each sample and used for diversity analyses. The Wilcoxon rank-sum test was used to compare the abundance of OTUs at different taxonomical levels; significant differences were identified after correction for false discovery rate. Statistical significance of sample groupings was tested with a multivariate non-parametric analysis of variance (adonis, 999 permutations) (Anderson, 2001). LDA Effect Size (LEfSe) (Segata et al., 2011) was used to identify taxa that discriminated microbiota profiles according to the diet.

qPCR Analysis of 16S rRNA genes

Quantitative PCR (qPCR) was used to enumerate bacterial 16S rRNA gene copies in the genomic DNA extracted from cecal, WAT and blood samples. Samples were quantified in 25 µl reactions containing 1x SYBR Green Master Mix (Thermo Scientific, Waltham, MA), 200 nM of each primer and 5 ng of genomic DNA. Standard curves for quantification consisted in ten-fold serial dilutions in the range of 10^8 to 10^0 copies of target 16S rRNA genes from reference strains, amplified with primers 27F (5'- GTTTGATCCTGGCTCAG-3') and 1492R (5'-CGGCTA CCTTGTTACGAC-3').

The total amount of bacterial DNA in WAT and blood samples was quantified with the universal primers UniF (5'-GTGSTGCAYGGYYGTCGTCA-3') and UniR (5'-ACGTCRTCCMCNCCTTCCTC-3') (Fuller et al., 2007) using the 16S rRNA gene of *Escherichia coli* W3310 as standard. In cecal samples, *Lactobacillus* with LactoF (5'-TGGAAACAGRTGCTAATACCG-3') and LactoR (5'-GTCCATTGTGGAAGATTCCC-3')

(Byun et al., 2004) and *Akkermansia* with AM1 (5'-CAGCACGTGAAGGTGGGGAC3') and AM2 (5'-CCTTGCGGTTGGCTTCAGAT-3'); the 16S rRNA genes of *Lactobacillus reuteri* SD2112 and *Akkermansia muciniphila* were used as standard, respectively. All measurements were performed in duplicates.

Measurement of TLR and NOD activation, SCFAs and LPS

Blood was collected from the *vena cava* of mice after an 4 h fast using a pyrogen-free syringe/needle, and plasma was immediately isolated and frozen in liquid nitrogen. TLR2, TLR4, TLR5, TLR9 and NOD2 agonists were assayed using HEK-Blue reporter cell lines expressing mTLR2, mTLR4, mTLR5, mTLR9 or mNOD2 (InvivoGen, San Diego, CA) using a modified version of the manufacturer's protocol. HEK-Blue cells were grown for two passages with medium supplemented with selective antibiotics provided by the manufacturer, and then passaged once in medium without any antibiotics. The assay was performed when cells were in passage 11-14 by plating 10^5 cells in 96-well plates containing 10% heat-inactivated (2 h at 56 °C) serum. Cells were then incubated with 2% (v/v) serum isolated from *vena cava* of fasted mice for 21 h at 37 °C under an atmosphere of 5% CO2/95% air. Twenty microlitres of the cell culture supernatants were added to 180 µl of the QUANTI-Blue substrate in a 96-well plate. The mixtures were then incubated at 37°C for 1-3 h and secreted embryonic alkaline phosphatase levels were determined using a spectrophotometer at 655 nm.

GC-MS was used for measurement of organic acids in caecal content samples from mice fed fish oil (N=6) and lard (N=6) based diets. 90 –140 mg of frozen caecal contents were transferred to glass tubes (16 × 125 mm) fitted with a screw cap, and a volume of 100 µl of internal standards stock solution (1M [1-^{13}C]acetate and [$^{2}H_6$]propionate, 0.5M [$^{13}C_4$]butyrate, 0.1M [1-$^{13}C_1$]isobutyrate and [1-^{13}C]isovalerate, [1,2-$^{13}C_2$]hexanoate, [^{13}C]lactate and [$^{13}C_4$]succinic acid each in 40 mM) was added to the tubes. Prior to extraction samples were freeze-dried at −50 °C for 3 h, yield 30–40 mg dry weight. Extraction, analysis and

quantification of the measured metabolites are described in detail by Ryan et al. (Ryan et al., 2014). LPS concentration in serum collected from *vena cava* was measured using Endosafe-MCS (Charles River, Lyon, France) based on the limulus amoebocyte lysate (LAL) kinetic chromogenic methodology as previously described (Caesar et al., 2012).

Immunohistochemistry of WAT

Immunohistochemistry on paraffin-embedded epididymal WAT sections (5 mm) was performed as previously described (Caesar et al., 2012). Cells were stained with MAC-2/galectin-3 antibody (CL8942AP, Cedarlane Laboratories, Burlington, ON) or CD45 antibody (ab25386, Abcam, Cambridge, UK) diluted 1:500. Adipocyte size, number of CLS and $CD45^+$ stained area were determined in histological sections of 15-50 mm^2 for each mouse. Adipocyte size and $CD45^+$ stained area were quantified using the software Biopix iQ 2.1.4 (Gothenburg, Sweden).

Microarray expression analysis

RNA was isolated from epididymal WAT using RNeasy Lipid Tissue Mini Kit (Qiagen, Hilden, Germany). 250 nanograms of total RNA from each sample were used to generate amplified and biotinylated sense-strand cDNA from the entire expressed genome according to the Ambion WT Expression Kit (P/N 4425209 Rev C 09/2009) and Affymetrix GeneChip® WT Terminal Labeling and Hybridization User Manual (P/N 702808 Rev 3, Affymetrix, Santa Clara, CA). The arrays (GeneChip® Mouse Gene 1.0 ST Array) were hybridized for 16 h in a 45°C incubator, rotated at 60 rpm, washed, stained and finally scanned using the GeneChip® Scanner 3000 7G according to the manufacturer's manual (PN 702731 Rev 3, Affymetrix).

The raw data were normalized using the robust multi-array average method (Li and Wong, 2001). Differential expression of microarray data was evaluated by Student's t-test followed by correction for false discovery rate. Analysis of interaction, using colonization status and

diet as independent variables, was evaluated by two-way analysis of interaction followed by correction for false discovery rate. Analysis of enrichment of regulated genes within functional categories [gene ontology categories (GO)] (Ashburner et al., 2000) was performed using the software David (Huang et al., 2008). The results of the enrichment calculation were filtered for GO categories that were significantly enriched ($p<0.05$) after Bonferroni correction. Redundancy within lists of GO terms was reduced by the Revigo software (Supek et al., 2011) with a similarity score set to 0.5. Principle component analysis was performed in MultiExperiment Viewer (MeV).

Quantitative RT-PCR

RNA was isolated from epididymal WAT using RNeasy kit with on-column DNase treatment (Qiagen). cDNA templates were synthesized from total RNA using the high-capacity cDNA reverse transcription kit (Applied Biosystems, Foster City, CA) according to the manufacturer's protocol. Primers used for *Tnfα* were CCAGACCCTCACACTCA (forward) and CACTTGGTGGTTTGCTACGAC (reverse) and primers used for *Ccl2* were AGGTCCCTGTCATGCTTCTGG (forward) and CTGCTGCTGGTGATCCTCTTG (reverse). PCR assays were performed in 25 µl reactions containing 1xSYBR Green Master Mix buffer (Thermo Scientific, Waltham, MA), and 900 nM gene-specific primers. Gene expression data were normalized to the ribosomal protein L32.

Primary cell harvest, cultivation and assays

Primary adipocytes were prepared by isolating preadipocytes from epididymal WAT of SPF mice fed standard chow diet. WAT was treated with collagenase type II (C6885, Sigma Aldrich, St Louis, MO) (10 mg/ml) in Hank's buffer supplemented with 2% BSA for 1 h at 37°C. The cells were run through a 70 µm cell strainer and the stromal vascular fraction was isolated by centrifugation. Erythrocytes were removed by ACK solution treatment.

Adipocytes were grown in ready-made mediums from ZenBio (OM-PM, OM-DM and OM-AM, ZenBio, Durham, NC) according to the manufacturer's protocol.

Primary macrophages were prepared by harvesting bone marrow from femur of SPF mice fed standard chow diet. Erythrocytes were removed by ACK solution treatment. Bone marrow cells were cultured in high-glucose Dulbecco modified Eagle medium supplemented with 10% FCS, 1% HEPES, 1% gentamycin, 0.01% β-mercaptoethanol, and 50 ng/mL M-CSF (416-ML-050, R&D Systems, McKinley Place, MN). Experiments were performed on differentiated macrophages after 10-12 days.

Primary cells were stimulated with 2% (v/v) of serum isolated from *vena cava* of fasted SPF or GF mice fed lard diet for 4 hours. The concentration of secreted CCL2 was determined by ELISA (MJE00, R&D Systems).

Supplementary References

Anderson, M.J. (2001). A new method for non-parametric multivariate analysis of variance. Austral Ecol *26*, 32-46.

Ashburner, M., Ball, C.A., Blake, J.A., Botstein, D., Butler, H., Cherry, J.M., Davis, A.P., Dolinski, K., Dwight, S.S., Eppig, J.T., et al. (2000). Gene Ontology: tool for the unification of biology. Nat Genet *25*, 25-29.

Byun, R., Nadkarni, M.A., Chhour, K.L., Martin, F.E., Jacques, N.A., and Hunter, N. (2004). Quantitative analysis of diverse Lactobacillus species present in advanced dental caries. Journal of clinical microbiology *42*, 3128-3136.

Caesar, R., Reigstad, C.S., Bäckhed, H.K., Reinhardt, C., Ketonen, M., Östergren Lundén, G., Cani, P.D., and Bäckhed, F. (2012). Gut-derived lipopolysaccharide augments adipose macrophage accumulation but is not essential for impaired glucose or insulin tolerance in mice. Gut *61*, 1701-1707.

Caporaso, J.G., Kuczynski, J., Stombaugh, J., Bittinger, K., Bushman, F.D., Costello, E.K., Fierer, N., Pena, A.G., Goodrich, J.K., Gordon, J.I., et al. (2010). QIIME allows analysis of high-throughput community sequencing data. Nat Methods *7*, 335-336.

DeSantis, T.Z., Hugenholtz, P., Larsen, N., Rojas, M., Brodie, E.L., Keller, K., Huber, T., Dalevi, D., Hu, P., and Andersen, G.L. (2006). Greengenes, a Chimera-Checked 16S rRNA Gene Database and Workbench Compatible with ARB. Applied and Environmental Microbiology *72*, 5069-5072.

Edgar, R.C. (2010). Search and clustering orders of magnitude faster than BLAST. Bioinformatics *26*, 2460-2461.

Faith, D.P. (1992). Conservation evaluation and phylogenetic diversity. Biological Conservation *61*, 1-10.

Fuller, Z., Louis, P., Mihajlovski, A., Rungapamestry, V., Ratcliffe, B., and Duncan, A.J. (2007). Influence of cabbage processing methods and prebiotic manipulation of colonic microflora on glucosinolate breakdown in man. Br J Nutr *98*, 364-372.

Haas, B., Gevers, D., Earl, A., Feldgarden, M., Ward, D., Giannoukos, G., Ciulla, D., Tabbaa, D., Highlander, S., Sodergren, E., et al. (2011). Chimeric 16S rRNA sequence formation and detection in Sanger and 454-pyrosequenced PCR amplicons. Genome Res *21*, 494 - 504.

Hamady, M., Walker, J.J., Harris, J.K., Gold, N.J., and Knight, R. (2008). Error-correcting barcoded primers for pyrosequencing hundreds of samples in multiplex. Nat Meth *5*, 235-237.

Huang, D.W., Sherman, B.T., and Lempicki, R.A. (2008). Systematic and integrative analysis of large gene lists using DAVID bioinformatics resources. Nat. Protocols *4*, 44-57.

Kleiber, M. (1932). Body size and metabolism. ENE *1*, E9.

Kozich, J.J., Westcott, S.L., Baxter, N.T., Highlander, S.K., and Schloss, P.D. (2013). Development of a dual-index sequencing strategy and curation pipeline for analyzing amplicon sequence data on the MiSeq Illumina sequencing platform. Appl Environ Microbiol *79*, 5112-5120.

Li, C., and Wong, W.H. (2001). Model-based analysis of oligonucleotide arrays: Expression index computation and outlier detection. Proceedings of the National Academy of Sciences *98*, 31-36.

Lozupone, C., and Knight, R. (2005). UniFrac: a new phylogenetic method for comparing microbial communities. Appl Environ Microbiol *71*, 8228 - 8235.

Price, M.N., Dehal, P.S., and Arkin, A.P. (2010). FastTree 2 – Approximately Maximum-Likelihood Trees for Large Alignments. PLoS One *5*, e9490.

Ryan, K.K., Tremaroli, V., Clemmensen, C., Kovatcheva-Datchary, P., Myronovych, A., Karns, R., Wilson-Perez, H.E., Sandoval, D.A., Kohli, R., Backhed, F., et al. (2014). FXR is a molecular target for the effects of vertical sleeve gastrectomy. Nature *509*, 183-188.

Salonen, A., Nikkila, J., Jalanka-Tuovinen, J., Immonen, O., Rajilic-Stojanovic, M., Kekkonen, R.A., Palva, A., and de Vos, W.M. (2010). Comparative analysis of fecal DNA extraction methods with phylogenetic microarray: effective recovery of bacterial and archaeal DNA using mechanical cell lysis. J Microbiol Methods *81*, 127-134.

Segata, N., Izard, J., Waldron, L., Gevers, D., Miropolsky, L., Garrett, W., and Huttenhower, C. (2011). Metagenomic biomarker discovery and explanation. Genome Biology *12*, R60.
Supek, F., Bošnjak, M., Škunca, N., and Šmuc, T. (2011). REVIGO Summarizes and Visualizes Long Lists of Gene Ontology Terms. PLoS One *6*, e21800.
Wang, Q., Garrity, G., Tiedje, J., and Cole, J. (2007). Naive Bayesian classifier for rapid assignment of rRNA sequences into the new bacterial taxonomy. Appl Environ Microbiol *73*, 5261 - 5267.
Vázquez-Baeza, Y., Pirrung, M., Gonzalez, A., and Knight, R. (2013). EMPeror: a tool for visualizing high-throughput microbial community data. GigaScience *2*, 16-16.
Zhang, J., Kobert, K., Flouri, T., and Stamatakis, A. (2014). PEAR: a fast and accurate Illumina Paired-End reAd mergeR. Bioinformatics *30*, 614-620.